APPLICATION OF THE VORTEX-LATTICE CONCEPT TO FLOWS WITH SMOOTH-SURFACE SEPARATION

by

David Fred Thrasher

Dissertation submitted to the Faculty of the
Virginia Polytechnic Institute and State University
in partial fulfillment of the requirements for the degree of
DOCTOR OF PHILOSOPHY
in
Engineering Mechanics

APPROVED:

Dean T. Mook, Chairman

William S. Saric

Mark S. Cramer

M. P. Kamat

Lee Johnson

March, 1984

Blacksburg, Virginia

APPLICATION OF THE VORTEX-LATTICE CONCEPT TO FLOWS WITH SMOOTH-SURFACE SEPARATION

by

David Fred Thrasher

(ABSTRACT)

A nonlinear three-dimensional vortex-lattice method which treats the steady separated flow over prolate bodies with open separation moving through an inviscid incompressible fluid is developed. The strength and position of the body wake are found as part of the solution. Specifically, flows with smooth-surface separation are considered as opposed to flows with sharp-edge separation treated with the vortex-lattice concept in the past. To demonstrate the technique, results for the flow over an inclinded ogive-cylinder are presented.

In the case of attached flow, comparsions are presented of the results from the vortex-lattice method using optimal and average control point locations with the results of the source-distribution method and with experimental data. Significantly, the same panel

arrangement is used in the calculations for both methods. The results demonstrate that the results of the present method is somewhat more sensitive to panel arrangement than are those of the source-distribution method. Also, the effect of control point location varies dramatically as the incidence of the body is changed.

In the case of separated flow, comparsions of the results of the vortex-lattice method are made with experimental data and with the results of a typical two-dimensional analogy. The results demonstrate that the present method agrees most favorably with the experimental data windward of a separation line.

Acknowledgments

It is difficult to overestimate the influence Professor Mook has had on my graduate and undergraduate education. Time is the most valuable gift one can give, and he gave generously. I should also mention his unsurpassed patience through the years. I shall always be indebted to him for sharing with me his keen insight in numerical analysis.

Almost all of the research presented here was done while I was employed with the Hydromechanics Branch, David Taylor Naval Ship Research and Development Center, Bethesda, Maryland. I thank my colleagues there for their encouragement and friendship. I wish to thank specifically my supervisors, Dr. Thomas Huang and Mr. Justin McCarthy, for the generous support and technical leeway that they constantly provided. This research was supported by the Naval Sea Systems Command Special Focus Program on the Separated Flow Field on a Submarine Executing a High-Speed Turn. The program's support is gratefully acknowledged.

I thank the members of my committee for their time and suggestions. Also, I would like to thank the entire mechanics faculty for their genuine interest in my education during my years at VPI.

My former wife, Pattie, put up with my endless nights at the office time after time. Her love and support through thick and thin are what made it all worthwhile. I feel just saying "Thank You" is so inadequate. May God bless her.

Russell supported me when the going was rough. I know I never would have finished except for his help.

I thank Dan Miller for his friendship and support since I have been with INCO.

Finally, the support and interest of my parents have always been there, and they made a difference. Though we have had some differences, my father has always been there to lend a hand. For that and another hundred or so reasons, this work is dedicated to him.

Table of Contents

Table of Contents (cont'd)

List of Figures

List of Figures (cont'd)

List of Figures (cont'd)

Chapter One

Introduction and Literature Review

The problem of potential flow separating from a smooth surface is of fundamental importance in fluid dynamics. In fact, one encounters smooth-surface separation in the potential flow over almost any body executing some maneuver of interest. Examples of problems with smooth-surface are the flows about:

- Missiles at angles of attack
- Wings at high angles of attack or yaw
- Aircraft fuselages
- Ship sterns

Recently, numerical schemes based on the vortex-lattice concept have had considerable success in treating the fully three-dimensional separated potential flow over low aspect-ratio thin wings at high incidence and the attached potential flow over bodies of more general shape. So far, separation has been constrained to take place along a sharp edge. However, in principle, the vortex-lattice method is not limited in application so long

as convection dominates vorticity diffusion.

We develop a nonlinear three-dimensional vortex-lattice method that treats the steady incompressible inviscid flow over bodies in cases where the separation takes place along a smooth surface. We assume that the flow does not reattach and vortex breakdown does not take place near the body. The location of the separation lines on the body are assumed known. The strength and shape of the body wake are found as part of the solution.

To demonstrate the feasibility of the technique, we present results for the flow over an inclined body with a tangent-ogive shaped nose and cylindrical afterbody, hereafter referred to as an 'ogive-cylinder'. The separation line used in the calculations begins aft of the ogive-cylinder junction and has a fixed circumferential location along the length of the body.

In the remainer of this chapter we discuss the flow topology and review similar efforts to solve the problem.

1.1 Toplogical Discussions

The first fundamental work concerned with the topological notions used here was done by Poincaré (1928) but we follow the more recent development of Peake and

Tobak (1980). We consider the flow about a smooth slender body inclined slightly to a uniform oncoming freestream. One of the streamlines in the oncoming flow attaches itself to the body near the nose at the forward stagnation point. The attachment point acts as a source of skin-friction lines which emerge and envelop the body. All of the skin-friction lines end at the rear stagnation point which acts as a sink for the lines. From this rear stagnation point a single streamline enters the external flow and extends downstream. The forward stagnation point is referred to as a 'nodal singular point of attachment' and the rear stagnation point as a 'nodal singular point of separation'.

An attached flow, then, is defined as a flow containing two and only two nodal points in the pattern of skin-friction lines. These are the nodal points of attachment and separation. We define a three-dimensional flow with more than two singular nodal points in the skin-friction line pattern as a 'separated flow'.

The simplest three-dimensional separated flow contains three nodal points, two being of the same type. Let us suppose that there are two nodal points of attachment and one nodal point of separation. The skin-friction lines emerging from the two attachment points must be prevented

from crossing. This requires another singular point between them, commonly known as a saddle point. One skin-friction line from each of the attachment points enters the saddle point and two skin-friction lines emerge. These emerging skin-friction lines act as separatices in the skin-friction line pattern. The other skin-friction lines tend to converge along either side of the separatrices. The separatrices are the separation lines on the body and they always emerge from a saddle point. The skin-friction line patterns of attached flows never contain any saddle points whereas the skin-friction line patterns of separated flows always contain at least one saddle point. We note that the convergence of skin-friction lines along either side of a particular skin-friction line does not necessarily constitute separation and that a skin-friction line emanating from a nodal point cannot be a separation line.

In this case there are three nodal points and one saddle point, making the difference between the number of nodal and saddle points two. It is a general rule that the number of nodal points in the skin-friction line pattern exceed the number of saddle points by two (Davey, 1961).

There is a surface extending from the body into the outer flow which originates along a separation line and prevents the boundary layer on either side of it from merging. The surface rolls up as it extends downstream and is the body wake. Vorticity generated within the boundary layer on the body is shed into the wake along a separation line.

Sears (1948) was among the first to introduce the concept of 'limiting streamlines' while discussing the laminar boundary layer on an infinite yawed cylinder. If we let the height of a streamline in the boundary layer on the body approach zero, the normal velocity tends to vanish faster than the tangential velocity. Thus, the resultant streamline or limiting streamline is parallel to the body and its projection onto the body surface is coincident with a skin-friction line.

Limiting streamlines have behaviour similar to that of skin-friction lines; that is, they emerge from nodal points of attachment, disappear into nodal points of separation, and converge along certain limiting streamlines that are parallel to separation lines. Sears included a sketch indicating this behaviour near a separation line but did not refer to it as such. Eichelbrenner (1954) and Eichelbrenner and Oudart (1955) proposed that a

three-dimensional separation line was the envelope of converging adjacent limiting streamlines.

Maskell (1955) suggested that the limiting streamlines on opposite sides of a separation line merged and left the surface as single streamlines on the 'surface of separation' (wake). He categorized simple separated flows into two classes: a 'closed' or 'bubble' type and an 'open' or shear-layer type. These are shown schematically in Figure 1-1. If the body is symmetric, the saddle point is located on the plane of symmetry for closed separation and off the plane of symmetry for open separation. In the case of open separation, fluid coming from upstream of the body wets both sides of the wake and the pressure is continuous across it.

Legendre (1956, 1965) and Oswatitsch (1957) independently showed that by viewing the pattern of limiting streamlines as a continuous vector field, the behaviour of the merging of streamlines called for in Maskell's discussion could not be accommodated. Reproducing their results and in a departure from his earlier work, Lighthill (1963) chose to work with skin-friction and surface-vortex lines. Both sets of lines cover the body completely, they intersect at right angles, and are unique everywhere. Moreover, the separation line

itself is a skin-friction line. Since the skin-friction lines are uniquely defined, their pattern can be viewed as a continuous vector field. He showed that the number and type of singular points on the surface obey topological rules. However, Legendre (1977) noted that as far as was then currently known, all experimentally determined skin-friction line patterns could be interpreted within the framework of his earlier work and that a more complicated singular-behaviour theory was not necessary to explain observed patterns.

The rules governing the number and type of singular points can be extended above the surface on planes of symmetry (Hunt, Abell, Peterka, and Woo, 1978), on projection of conical flows (J.H.B. Smith, 1969) and on cross-flow planes (Perry and Fairlie, 1974).

We now turn to a discussion of other attempts to treat the problem of interest.

1.2 Two-Dimensional Approaches

A large number of methods treat the separated flow over a prolate body by means of a two-dimensional analogy. Typically, the three-dimensional steady problem is related to the solution of a two-dimensional time-dependent problem. The two-dimensional unsteady problem is solved

and then an approximate solution of the three-dimensional problem inferred.

Many two-dimensional methods employ the 'cross-flow plane' or 'impulsive flow' analogy, first suggested by Allen and Perkins (1951). These methods consider the impulsively started flow over a cylinder to be analogous to the flow in a plane perpendicular to the body's longitudinal axis. Time in the former problem is related to the axial distance of the cross-flow plane in the latter problem. Hence, the task remains to find the two-dimensional time dependent flow over a cylinder experiencing impulsively started flow.

The most rigorous formulations using this approach numerically solve the Navier-Stokes equations for the impulsive flow over the cylinder. Thoman and Szewczyk (1969) and Jordan and Fromm (1972) treated the flow over an inclined cylinder in this manner while Walitt and Trulio (1971) considered the compressible flow over an inclined body of revolution. Unfortunately, the computational requirements for this approach can be prohibitive due to the Navier-Stokes integration.

Less rigorous and more practical formulations employing the cross-flow plane analogy use the 'discrete-vortex' method to obtain the impulsive flow solution. Originally developed by Rosenhead (1932), the discrete-vortex method is based on replacing the Karman vortex streets behind the moving cylinder with point vorticies. Time is discretized and marched in a pedestrian fashion. At each time step, a new point vortex is introduced in the outer flow at each separation point. The vorticies in the wake subsequently travel downstream under their mutual influence.

The discrete-vortex method is plagued with a number of numerical problems, however. Birkhoff and Fisher (1959) and Hama and Burke (1960) repeated Rosenhead's calculations and found that increasing the number of vorticies tracked in the wake often led to their chaotic motion. Fink and Soh (1974) developed a rediscretization procedure whereby the vorticity in the wake is redistributed among the vorticies at each time step. However, Baker (1980) claimed that their test case was inadequate and that their error estimate was suspect. Baker used their technique to study the wake behind a ring wing and found that the discrete-vortex method still predicted physically

unrealistic results as the number of vorticies was increased when using Fink and Soh's modification. Baker could not arrive at a definitive reason for the breakdown although it appears that he did not reduce the temporal step size in a consistent manner as he increased the number vorticies tracked in the wake. In any case, such a rediscretization process in three dimensions would probably be unmanageable.

There are a number of empirical factors in the discrete-vortex formulation as well. For example, the predicted strength of the vorticies shed into the wake must be reduced significantly for realistic results. Schoaff (1978) and Sarpkaya and Schoff (1979) decreased the strength of the vorticies gradually as they travelled downstream in an effort to simulate the dissipation and diffusion of vorticity. The shape and size of their dissipation function was guided by numerical experimentation. Significantly, they solved for the separation angle numerically and found it to agree favorably with experiments.

The cross-flow analogy, in combination with the discrete-vortex method, has been used to calculate the flow over bodies at incidence with varying degrees of success. Unfortunately, the approach requires empirical guidance and

considerable artwork on the part of the user. For examples of the discrete-vortex method and its application, see Sarpkaya (1966), Gerrard (1967), Sarpkaya (1968), and Laird (1971).

A similar approach using the cross-flow plane analogy uses a lumped vortex cross-flow model (Bryson, 1959). Here, a point vortex is joined to the body with a feeding sheet of negligible strength. The system is then adjusted such that it is globally force-free with the force on the feeding sheet balancing the force on the point vortex. The force per unit of length on the body is equal to the time rate of change of the momentum in the cross-flow plane. Schindel (1965, 1969) used conformal mapping to extend this method to bodies with elliptic cross-sections while Wardlaw (1973) calculated side forces on bodies combining asymmetric vorticies and slender-body theory.

In a modification of Bryson's model, called the multi-vortex model, a number of free point vortices were allowed to roll up and form a concentrated vortex in each cross-flow plane. Angelucci (1971) and Marshall and Deffenbaugh (1974) treated bodies with symmetric vortex shedding in this way while Wardlaw (1975) extended the method to treat asymmetric vortex shedding. Angelucci calculated the force distribution using the vortex impulse

theorem while Wardlaw used a momentum balance similar to Bryson. Marshall and Deffenbaugh calculated and then numerically integrated the circumferential pressure distribution to find the normal-force coefficient on the body. They also solved for the boundary-layer flow numerically using two-dimensional criteria to determine the location of the separation lines on the body.

Thompson and Morrison (1971) found that analyzing the wake behind an inclined cone-cylinder by means of the impulsive flow analogy led to reasonable predictions of the Strouhal number but the vortex strength was over-estimated. However, they found that the Karman vortex street theory combined with the vortex sweepback principle led to satisfactory predictions of the vortex strength. In the sweepback principle, the wake is considered to be part of a steady infinite vortex street. The vortex street velocity is then cancelled by the component of the freestream normal to the vortex lines. In the application of the principle, it is important that the cross-flow component of the freestream can be considered incompressible. Kubin (1973), Fidler and Bateman (1975), and Kao (1975) use this approach with minor variations to account for the nose vorticies which do not follow the pattern of a Karman vortex street. The Thompson and Morrison correlations provided the required empirical data.

While these two-dimensional approaches are by no means completely adequate to model the complicated picture of a general three-dimensional separated flow, it is intriguing that they can provide us with more than just qualitative details of the flow. Several engineering problems have been solved using the cross-flow plane analogy. It is perhaps important to note that the topologies of two-dimensional unsteady and three-dimensional steady flows appear analogous (Tobak and Peake: 1981a, 1981b). A stricter correspondence between the two problems is certainly with some doubt. For example, the growth of an unsteady two-dimensional vortex differs in important ways from the development of a steady three-dimensional vortex structure. In three dimensions, the fluid entering the core of the vortex can be discharged axially whereas in two dimensions such an escape is not possible. Thus, a two-dimensional vortex must expand to accommodate fluid entering the core region. Only in one case are the two kinds of vortex flows formally identical: a steady, three-dimensional conical vortex and an unsteady two-dimensional vortex that grows linearly with time. See Peake and Tobak (1980) for a discussion of the issue of two-dimensional and three-dimensional vortex correspondence.

Another important issue dealing with two-dimensional analogs is the lack of upstream influence. The upstream influence in the flow is more pronounced when the body's radius varies along the length of the body. One attempt to account for the expanding radius of the body as one moves axially along the nose is to assume that the cylinder being modeled in the impulsive flow analogy is expanding. The expansion rate is related to the number of cross-flow planes used in the calculation and to the speed and incidence of the body.

1.3 Three-Dimensional Approaches

1.3.1 Attached Flows

The fundamental problem of the three-dimensional attached flow over an arbitrary body has been treated by a number of authors. By far, the most popular and successful of these methods have been integral-equation methods. These methods express the solution of the problem in terms of an integral equation which is then treated numerically. They differ from one another mainly in the form of the kernel and the numerical procedure used to obtain a solution. Integral-equation methods effectively reduce the three-dimensional problem to a two-dimensional one as the velocity (or velocity potential) need only be calculated on

the body and wake surfaces, not in the complete external flow. However, only with the advent of high-speed computers have these methods proved practical.

The use of an integral-equation method can be broken up into two main parts. First, the form of the integral-equation form must be chosen. This is equivalent to choosing the type of singularity (e.g. sources, doublets, vorticies, etc.). Second, the solution procedure and boundary-condition form (Neumann or Dirichlet) must be specified.

Typically, a Neumann boundary condition (i.e., no penetration through the body surface) is enforced in a collocation manner. The collocation points are referred to as 'null' or 'control' points. A set of linear algebraic equations is written for the strengths of a finite number of discrete singularities on or near the body surface. Upon solution, the fluid velocity (or velocity potential) is evaluated and the pressure coefficient determined at each control point.

One of the earliest integral-equation methods is that of Hess and Smith (1962, 1964, 1966). Here, a distribution of flat quadrilateral source panels of constant strength are placed near the body surface in the manner described by Kellogg (1929). The strength of each source panel is

determined, and the velocity potential is calculated at each control point. Numerical differentiation along the body surface yields the fluid velocity at each control point. Bernoulli's equation is then used to calculate the pressure coefficient. Landweber and Macugno (1969) modified the method in the treatment of the singularity of the kernel in the numerical procedure. Webster (1975) developed a method using triangular source panels of linearly varying strength. In his model,the source strength was continuous across panel edges. In an effort to reduce surface velocity irregularities, he submerged the singularity surface beneath the body surface as was done previously by Pien (1964). The method calculated relatively smooth velocity variations on the body surface and allowed for fairly accurate calculation of streamlines.

Chang and Pien (1975) used a distribution of doublets on the body surface in a method similar to the aforementioned source-distribution methods. Johnson and Rubbert (1975) combined sources and doublets in a higher-order method which enforced either a Neumann or Dirichlet boundary condition on the velocity potential in a collocation manner. The source strength for each panel was prescribed to cancel the component of the freestream velocity normal to the panel. They found that using a Dirichlet boundary condition resulted in remarkable

insensitivity of the results to panel arrangement.

Asfar (1978) treated the flow over bodies of general shape with a surface distribution of vortex segments (a vortex-lattice method). In the vortex-lattice method, the fluid velocity at the control points is calculated directly from the singularity strengths rather than differentiating the velocity potential. Asfar, Mook, and Nayfeh (1978) showed that combining sources of known strengths with the vortex-lattice method resulted in more accurate pressure distributions over bodies of simple shape. In this case, the source strengths were adjusted to cancel a portion of the normal component of the freestream velocity for each panel.

In all the methods mentioned thus far, the strength of an auxiliary singularity distribution is first obtained by construction of a large influence coefficient matrix. Then, the velocity (or velocity potential) is calculated on the body by solving a set of simultaneous linear equations. Another approach is to solve for the singularity distribution on the body in an iterative fashion. The key advantage in this alternative method of solution is that far less computer storage is required and often the iterative procedure can be shown to converge rapidly for problems of interest. Among the first to apply

the iterative approach to fluid flow problems was Chow, Hou and Landweber (1976). Chow, Lee, and Owen (1982) used an iterative approach to solve for the source distribution on a body while Noblesse (1983) and Noblesse and Triantafyllou (1983) developed a method to solve iteratively for the velocity potential on the body. Among the attractive features of Noblesse's technique is that especially rapid convergence was proved for the case of longitudinal translation of a slender or thin body. It also can be extended to treat free-surface flow problems.

1.3.2 Separated Flows

The three-dimensional flow over thin wings with sharp-edge separation has been treated with nonlinear vortex-lattice methods by a number of authors over a wide variety of planforms. Steady flows were considered by Mook and Maddox (1974); Kandil (1974); Kandil, Mook, and Nayfeh (1976); as well as Zorea and Rom (1978). Kelly (1977) presented a valuable parametric study of the steady nonlinear vortex-lattice method for thin wings.

Kandil, Chu, and Yates (1980) describe a 'Hybrid' vortex-lattice method whereby a continuous-vorticity model is used for near-field velocity calculations and a discrete-vortex model (such as the one used here) for

far-field calculations. The method's feasibility was investigated and some preliminary results presented but significant work remained to be done. Yen, Mook, and Nayfeh (1981) developed a continuous-vorticity panel method enforcing continuity of vorticity strength across panel edges. Their results were encouraging.

Nikolitsch (1978) treated wing-body combinations by combining Wardlaw's version of Bryson's vortex line model with Gersten's (1961) nonlinear lifting-surface theory for wings. Wing-body combinations were also treated by Uchiyama, Mikkilineni, and Wu (1978) using distributed sources on the surface of the body and a nonlinear vortex-lattice method to model the wings. They attached a straight semi-infinite vortex line on either side of the nose of the body. The attachment points and strength of each of the vortex lines were empirically estimated. Sheffield and Deffenbaugh (1980) used the same approach to treat simple bodies at incidence but solved for the shape of the vortex lines as well.

Atta (1978) and Atta and Nayfeh (1978) solved for the flow over wing-body combinations using a vortex-lattice method for both the body and the wings. They allowed for separation off the sharp edges of the wing only.

Maskew, Rao, and Dvorak (1980) and Maskew (1981) used a combination doublet-lattice and source-distribution method enforcing a Dirichlet boundary condition to solve for the flow over thick wings where flow separation was not confined to the edges of the wing and thus treated a problem similar to the one we consider here.

Fiddes (1980) solved for separation angle on a cone at incidence by interacting F.T. Smith's (1978) extension of the two-dimensional triple-deck boundary-layer theory of Sychev (1972) with a sophisticated vortex-sheet model. Fiddes represented the vortex sheets as a series of circular arcs which meet tangentially at their end points. Their application was somewhat limited as Fiddes employed slender-body and conical flow assumptions and his boundary-layer method was limited to laminar flows.

Rehbach (1977) presented an entirely different approach to represent three-dimensional vortex flows adopting a Lagrangian view of the circulation shed from a separation line. He used a vortex lattice on the wing surface but integrated the vorticity transport equation in the wake. There was some difficulty in matching the two presentations of vorticity along the separation line which he described as 'delicate'.

1.4 Summary

In this chapter we introduced the topic of discussion and briefly reviewed the recent literature pertaining to the problem. More complete general reviews of three-dimensional separated flows are given by J.H.B. Smith (1975, 1977, 1980), Peake and Tobak (1980), and Tobak and Peake (1981a, 1981b).

In a departure from earlier work, we present a vortex-lattice method that treats the flow over bodies with separation along a smooth surface. Earlier vortex-lattice methods either treated attached flows or constrained separation to take place along sharp edges. We compare the results of the vortex-lattice and source-distribution methods. In the calculations, the same lattice configuration was used for both methods. To our knowledge, this is the only published comparison of the two methods where calculations where performed using precisely the same lattice layout. We also show that the effect of control point placement varies significantly with incidence. This discovery sheds new light on some modifications to the vortex-lattice method which were only tested at zero incidence for original publication.

In Chapter Two, we make a mathematical statement of the problem and develop a hydrodynamic model based on continuous sheets of vorticity.

In Chapter Three, we develop a numerical model, based on the vortex-lattice concept, to accompany the hydrodynamic model.

In Chapter Four, we compare the results of the method with those of other methods and experiments and investigate several numerical phenomena as well.

In Chapter Five, we make conclusions about the work and recommendations for further areas of study.

Chapter Two

Hydrodynamic Modeling

We consider the steady inviscid incompressible flow over a body at an angle of attack. The fluid moves with a uniform freestream velocity far from the body and its extent is infinite. The angle of attack is sufficient to develop large scale separation on the leeside of the afterbody but not so large as to precipitate unsteady vortex shedding. Any asymmetry in the flow is due to geometry rather than to flow instabilities. Reattachment and secondary separation effects are neglected.

2.1 Bound- and Free-Vortex Sheets

When the flow separates, vorticity generated within the boundary layer on the body is shed into the outer flow along separation lines. This shed vorticity forms the body wake. The resulting flow is fully three-dimensional and nonlinear. The wake shape and strength are important in determining the flow field surrounding the body and ultimately the loads.

If the Reynolds number is high, the wake is thin when compared with the overall dimensions of the body. Consequently, the vorticity in the flow is concentrated into the thin boundary layer on the body and the thin vortical regions comprising the wake. The flow outside these regions is essentially irrotational. We pose the problem in terms of the strength of the vorticity distribution and the shape of the body wake.

We can express the velocity field, $\vec{V}$, at a field point located by the position vector, $\vec{r}$, in terms of the vorticity distribution, $\vec{w}_\tau$, for any incompressible flow as (see Karmacheti, 1966, Chapter 9):

$$\vec{V}(\vec{r}) = \frac{1}{4\pi} \operatorname{curl} \iiint_{\tau} \frac{\vec{w}_\tau(\vec{q})}{\left[\vec{r} - \vec{q}\right]^3} \, d\tau \qquad (2.1)$$

where q is the position vector locating the volume element $d\tau$ with associated vorticity $\vec{w}_\tau(\vec{q})$, the integration is performed over the volume of the vortex field, τ , and the curl is taken with respect to the components of $\vec{r}$.

The regions of non-zero vorticity are thin everywhere. This leads us to let the representative thickness of each of these regions, ϵ , tend toward zero and simultaneously to let the strength of the vorticity tend to infinity in such a manner that the far-field influence remains the

same. While taking the limit, the product of the thickness and the strength of the vortex sheet remains constant. Thus, the boundary layer on the body becomes a bound-vortex sheet and the thin wake regions each become free-vortex sheets. We define the surface vorticity distribution, $\vec{w}_s$, on these vortex sheets as:

$$\vec{w}_s(\vec{q}) = \lim_{\substack{\epsilon \to 0 \\ w_\tau \to \infty}} \epsilon \vec{w}_\tau(\vec{q}) \qquad (2.2)$$

We now integrate (2.1) over the thickness and obtain:

$$\vec{V}(\vec{r}) = \frac{1}{4\pi} \text{curl} \iint \frac{\vec{w}_s(\vec{q})}{\left[\vec{r} - \vec{q}\right]^3} ds \qquad (2.3)$$

where the position vector $\vec{q}$ now locates the area element ds and the integration is performed over the combined surfaces of the bound- and free-vortex sheets. The problem remains to specify the shape of the free-vortex sheet and the vorticity distribution on the bound- and free-vortex sheets.

2.2 Kinematic Flow Conditions

There are a number of conditions that the solution must satisfy. First, there must be no penetration through the body surface. We write that:

$$\vec{V} \cdot \vec{n} = - \vec{V}_{\infty} \cdot \vec{n} \qquad (2.4)$$

where $\vec{V}_{\infty}$ is the undisturbed freestream velocity, $\vec{V}$ is the disturbance velocity, and $\vec{n}$ is the unit normal to the body surface.

Second, vorticity is a divergenceless field by construction or:

$$\text{div}(\vec{w}) = \text{div}\ (\text{curl}\ \vec{V}) = 0 \qquad (2.5)$$

Furthermore, according to the Kelvin-Helmhotz theory of vorticity, the substantial derivative of circulation, Γ, on a free-vortex sheet is zero or:

$$\frac{D\Gamma}{Dt} = 0 \qquad (2.6)$$

Consequently, free vorticity is convected downstream with the local particle velocity. Thus, a steady free-vortex sheet is a stream surface.

2.3 Separation Line Conditions

We must specify conditions along the separation lines as well. Since we are posing our problem in terms of a vorticity distribution, we seek a condition on the strength of vorticity along a separation line. J.H.B. Smith (1980) showed that the inviscid streamlines just leeward and windward of a separation line are parallel and inclined to

the separation line, respectively. The windward streamlines then leave the body surface and vorticity generated in the boundary layer is swept into the outer flow along them. It follows that nonzero bound vorticity along a separation line would generate a crossflow relative to the separation line on the surface of the body. Since the streamlines just leeward of a separation line are parallel to the separation line, we set the bound-vortex strength coincident and parallel to a separation line to zero. Spatial conservation of vorticity demands that this vorticity be swept into the outer flow where it travels downstream to form the body wake.

2.4 Summary

In this chapter we have discussed the approximation of steady separated flow over a body by a continuous vortex-sheet model. It remains to solve for the shape of the free-vortex sheets and the vorticity distribution everywhere subject to the following conditions:

1. There is no penetration through the bound-vortex sheet.
2. Vorticity is divergenceless or alternatively there is spatial conservation of circulation.
3. Free vorticity is convected downstream at the local particle velocity.
4. Bound vorticity coincident with a separation line

vanishes. The requirement of spatial conservation of circulation then dictates the strength of the wake.

In the next chapter we present a numerical model for the hydrodynamic model presented here.

Chapter Three

Numerical Modeling

In this chapter, we present a numerical model and solution procedure to accompany the hydrodynamic model presented in Chapter Two. The model is based on the vortex-lattice concept of replacing continuous vortex sheets with arrangements of vortex segments. The placement of the vortex segments on the vortex sheets is guided by the physics of the flow. We replace the bound- and free-vortex sheets with lattices of short straight vortex segments. The position of the segments in the free-vortex sheet and the strength of the segments in both the bound- and free-vortex sheets are then found by a nonlinear iteration procedure.

We first describe the modeling of the bound-vortex sheet and explain the procedure for solving for the attached flow over the body. Next, we describe the modeling of the free-vortex sheets and outline the iteration procedure for solving for the separated flow over the body. We then discuss velocity calculations, the solution of the arising set of simultaneous linear

equations, the iteration process to render the wake force-free, and finally the calculation of the loads on the body. Many of the concepts introduced in this chapter are illustrated further in the next chapter with numerical examples.

3.1 The Bound-Vortex Lattice

We begin by replacing the continuous bound-vortex sheet with circumferential and longitudinal families of curved vortex lines which lie on the body's surface. The longitudinal vortex lines start at the nose of the body and continue back to the body's tail. The circumferential vortex lines form a series of axially spaced vortex rings which enclose the body. These two families of vortex lines intersect at various nodes to form rows and columns of vortex panels or elements which cover the entire body. The vortex lines are placed such that the resulting arrangement of vortex panels is regular and uniform. The panels that meet to form the nose and tail are three-sided and the remaining panels are four-sided. Such an arrangement is show schematically in Figure 3-1.

Short curved vortex segments which connect the various nodes on the body act as edges of the vortex panels. We replace these curved segments with straight segments which

the connect the same nodes. The panels now have straight sides. These straight vortex segments make up the bound-vortex lattice.

The three-sided vortex panels are flat. The four-sided vortex panels are nonplanar, in general, because all four corners need not lie in the same plane. In practical applications, however, the four-sided panels are almost flat. Thus, we calculate the panel area and normal direction for a nonplanar panel as though it were flat. The normal direction of a panel is parallel to the cross product of the panel's diagonals and its area is equal to one-half the magnitude of the same cross product.

We satisfy the no-penetration condition on the body using a collocation procedure. That is, we enforce the no-penetration condition at a finite number of discrete points on the body and do not satisfy it elsewhere. (Indeed, large unrealistic normal velocities are induced between collocation points.) We call these collocation points 'control points' and place one on each panel.

We choose to place the panel's control point on a plane that contains the centroid of the corners of the panel and is perpendicular to the panel's normal. We refer to this plane as the panel plane. If the panel is nonplanar then the panel's centroid usually will not lie on

the panel surface nor will the panel plane contain any of the panel's corners.

In their distributed source method, Hess and Smith (1962) define a panel plane for each panel in the same manner as we do here and then project the panel's corners onto the panel plane along a direction parallel to the panel's normal. Thus, the corners of adjoining panels are not necessarily coincident as they are here.

We explore two choices for the placement of the control point on a panel plane. The first choice, used by most authors, is to place the control point at the panel's centroid. We refer to this set of control points as 'average' control points. A second choice, investigated by Kelly (1977) and used by Asfar, Mook, and Nayfeh (1978), is the point on the panel plane of minimum normal velocity induced by a unit loop circulation (defined below) around the panel. These control points are referred to as 'optimal' control points, and their use can have a profound effect on the results obtained, as shown in the next chapter.

We refer to the circulation around a vortex segment as a 'branch' circulation and denote it with the symbol 'Γ'. Its sign and associated direction is taken according to the right-hand rule.

Each vortex segment replaces the surface vorticity component parallel to it and in an area immediately surrounding it. Thus, longitudinal segments replace the longitudinal components of vorticity on the body surface and likewise for the circumferential direction. Figure 3-2 illustrates this concept. We see that the longitudinal component of vorticity in shaded area 'A' is replaced by the vortex segment 'a' while the circumferential component of vorticity in shaded area 'B' is replaced by the vortex segment 'b'. If the two panels bordering a vortex segment have equal areas then the segment receives one-half of its strength from each of those panels. That is, the vortex segment's strength originates equally from each of the panels the segment borders. However, if the two panels have areas which are widely different then more of the segment's strength originates from the panel with the larger surface area. In an attempt to account for this discrepancy, we weight the branch circulations with the appropriate panel areas when approximating the vorticity vector, $\vec{w}$, associated with a vortex panel or:

$$\vec{w} = \frac{1}{A} \sum_{i=1}^{m} \frac{\Gamma_i \vec{l}_i A}{(A + A_i)} \qquad (3.1)$$

where i is the side of the panel,

$\vec{l}_i$ denote the vectors connecting consecutive nodes of the panel,

Γ_i denotes the branch circulations of the corresponding vortex segments,

A denotes the panel area,

A_i denotes the area of the adjacent panel on the i-th side,

and m is the number of panel edges (either three or four).

When the branch circulations used in the pressure calculations are calculated with this area weighting, we refer to them as 'area-weighted' circulations. When the branch circulations are calculated using equal contributions from each of the neighboring panels, we refer to them as 'equally-weighted' circulations.

As demonstrated in the next chapter, weighting the branch circulations helps alleviate some of the problems normally encountered with irregularly spaced lattices.

In this formulation the vorticity strength is constant across each panel and is discontinuous along panel edges. A higher-order formulation would allow the vorticity strength to vary across each panel surface and be continuous to some degree along the panel edges.

Spatial conservation of vorticity (or alternatively, circulation) demands that the sum of the branch circulations at any node in a vortex lattice vanish. A convenient a to satisfy this requirement is to define the branch circulations in terms of loop circulations. This is analogous to the familiar loop and branch currents used in the analysis of electrical networks. We denote loop circulations with the letter 'G'. In Figure 3-3 we see that the branch circulation 'Γ' for the vortex segment bordering panels labeled 'i' and 'i+1' is given by:

$$\Gamma = G_{i+1} - G_{i} \tag{3.2}$$

We solve for the loop circulations as primary variables. We then immediately write the branch circulations as algebraic combinations of the loop circulations. We use the Biot-Savart law to calculate the velocity field due to an individual vortex segment with its associated branch circulation (see Section 3.5). To find the velocity at a field point we add the freestream

velocity to the combined velocity due to all the vortex segments in the flow.

3.2 The Attached Flow Solution Procedure

To enforce the no-penetration condition, we write a set of simultaneous linear equations for the loop circulations, or:

$$\sum_{j=1}^{N} A_{ij} G_j = -\vec{V}_\infty \cdot \vec{n}_i \quad \text{for } i = 1,2,\ldots,N \qquad (3.3)$$

where i denotes the panel number,

A_{ij} are the influence coefficients,

$\vec{V}_\infty$ is the undisturbed freestream velocity,

$\vec{n}_i$ is the unit normal for panel 'i',

and N is the number of panels on the body.

The influence coefficient A_{ij} is equal to the normal velocity induced at control point 'i' due to a unit loop circulation around panel 'j'. The solution of (3.3) is addressed in Section 3.6.

In the case of attached flow, once the no-penetration condition is satisfied we can calculate the loads on the body as described in Section 3.8.

3.3 The Free-Vortex Lattice

We use free-vortex lattices to replace the continuous free-vortex sheets in much the same way as we use a bound-vortex lattice to replace the bound-vortex sheet. Each free-vortex sheet joins the bound-vortex sheet along a prescribed separation line.

We first arrange the bound-vortex lattice such that each separation line coincides with one of the longitudinal vortex lines on the body. Furthermore, we place the circumferential vortex lines such that each separation line on the body begins and ends on a node. Such an arrangement is only possible when the separation line's circumferential variation is small. The arrangement is shown schematically in Figure 3-4.

We place a number of semi-infinite non-intersecting curved vortex lines on each of the free-vortex sheets. Each wake vortex line emanates from a node on the bound-vortex lattice on a separation line and extends downstream parallel to a streamline. These wake vortex lines divide each free-vortex sheet into streamwise strips or 'ribbons' of surface vorticity. The vorticity distributed on each of these wake ribbons is subsequently concentrated into the vortex lines which border it in a similar fashion as the bound vorticity is concentrated into

the bound-vortex segments.

We replace each curved vortex line in the wake with a number of short straight connected vortex segments. The first segment in each wake line attaches to the bound-vortex lattice and the remainder extend downstream a finite distance. At the end of the last segment for each line we place a straight semi-infinite vortex line which extends downstream parallel to the undisturbed freestream.

The separation line condition demands that the bound vorticity coincident with a separation line vanish. In view of the role the longitudinal bound-vortex segments play in modeling the bound vorticity, we set the circulation around each of the longitudinal vortex segments along a separation line to zero. Spatial conservation of circulation determines the strength of the free-vortex segments. We include the wake lines in the calculation of the influence coefficients which correspond to the panels which border a separation line. This makes the influence coefficient matrix a function of the wake shape.

The problem remains to determine the orientation of the first wake segment in each line. J.H.B. Smith (1978) has shown that a free sheet leaves the body tangentially as the Reynolds number approaches infinity. We are unable to allow the sheet to do this however due to numerical

difficulties with the singular nature of vortex lines. To circumvent this problem at present we simply place the first segment in each wake line perpendicular to the body and make it short.

The Kelvin-Helmhotz theory of vorticity requires that free vorticity travel downstream with the local particle velocity. Thus, each wake vortex line is actually a streakline. If we view the steady state solution as a typical time step in the solution of the more general unsteady problem with steady flow conditions, each of the finite wake vortex segments represents an Euler step in the time integration of the path followed by a fluid particle. We align each finite wake vortex segment with, and make its length proportional to the local particle velocity. This provides for a force-free wake. The proportionality constant is the time increment, which we choose to be unity. We use the velocity at the upstream end of a wake segment for directing and sizing the segment. Kelly (1977) investigated using other points along the segment and found that the fewest iterations were required using the upstream end and that the predicted loads were best as well. Schroder (1978) used the average of the velocities calculated at the upstream and downstream ends but this practice almost doubles the computer time necessary for solution and the results were not significantly different

from those obtained by using the upstream end.

3.4 The Separated Flow Solution Procedure

Our task is to find the position of each finite vortex segment in the wake and the set of loop circulations that simultaneously enforce the no-penetration condition on the body and render the wake force-free. We use the following iteration procedure:

1. Preset the wake position.
2. Calculate the influence coefficient matrix.
3. Solve for the loop circulations which enforce the no-penetration condition.
4. Position the wake vortex segments so that they are force-free.
5. Repeat steps 2-4 until convergence is achieved.

In step one, we set the wake position to be either flat or obtain it from a previous solution. Step two involves changing only those columns in the influence coefficient matrix which correspond to panels bordering a separation line. Steps three and four require more elaborate calculations and are discussed in Sections 3.6 and 3.7.

3.5 Velocity Calculations

We calculate the velocity field due to a vortex segment using the Biot-Savart law (see Karamcheti, 1966). For a single straight vortex segment of strength ' ', the velocity at field point 'P' is given by the following computationally advantageous form (see Figure 3-5):

$$\vec{V}_p = \frac{\Gamma}{4\pi} \frac{\vec{r}_{12} \times \vec{r}_1}{\left| \vec{r}_{12} \times \vec{r}_1 \right|^2} \left[\vec{r}_{12} \cdot \left(\frac{\vec{r}_1}{\left| \vec{r}_1 \right|} - \frac{\vec{r}_2}{\left| \vec{r}_2 \right|} \right) \right] \quad (3.4)$$

The velocity due to a vortex segment tends to infinity as the field point approaches the segment. To avoid this physically inconsistent behaviour, we insert a 'viscous' core around the segment where the induced velocity is zero.

3.6 The Solution of Simultaneous Linear Equations

An efficient solution of the arising set of simultaneous linear equations is important in solving for the flow over the body. This is especially true in the case of separated flow since we must do it once for every iteration between the wake position and loop circulations.

In general, iterative methods are particularly well suited for solving linear systems of equations when a good initial guess is available or when the number of equations prohibits its complete storage in high-speed memory. For an iterative method we use the modified Gauss-Seidel method (Johnson and Riess, 1977) or the modified Gauss-Seidel method with successive overrelaxation, sometimes called the SOR method (Goult, Hoskins, Milner, and Pratt, 1974).

In contrast, direct methods are particularly well suited for solving linear systems of equations when a good initial guess is not available or when the number of equations allows for complete storage in high-speed memory. For a direct method, we use the Gauss-elimination method with partial pivoting (Johnson and Riess, 1977).

The number of operations (multiplications and divisions) for the Gauss-Seidel method is $O(N^2)$ per iteration while the Gauss-elimination method requires $O(N/3)^3$ operations for complete solution. Of course, with the direct method, considerable row exchanges may be necessary if pivoting is used. Row exhanges do not require significant additional computation if row indexing is used, however.

A number of factors determine the structure and conditioning of [A] and thus govern the choice of solution scheme. By inspection, we can show that if the body is closed, for any row 'i' in [A]:

$$\sum_{j=1}^{N} A_{ij} = 0 \qquad (3.5)$$

Thus, every column of [A] is a linear combination of the remaining columns and the matrix is singular. This is because the loop circulations are the unknowns in the problem while the branch circulations determine the velocity field. Since each of the branch circulations is defined as the difference between two of the loop circulations, the set of loop circulations which induce a particular velocity field are unique only within an additive constant or functionally:

$$\vec{V}([G]) = \vec{V}([G] + s[C]) \qquad (3.6)$$

where 's' is a scalar and [C] is a vector of ones and is of the same length as [G].

If the body is not closed then we can show that for any row 'i' in [A]:

$$\sum_{j=1}^{N} A_{ij} = d_i \qquad (3.7)$$

where d_i is the velocity induced normal to control point 'i' due to a unit branch circulation around each of the vortex segments which border an opening.

For those rows which correspond to panels far away from any opening, d_i can be $O(10^{-4})$ but it grows rapidly as we move towards an opening. Even though the matrix is no longer singular, we found that partial pivoting was necessary for the Gauss-elimination method to obtain a solution.

While using the modified Gauss-Seidel method, we found that after several iterations, successive iterates of the loop circulations in both the singular and non-singular cases could be approximated by:

$$[G]^{k+1} = [G]^{k} + s^{k} [C]^{k} \qquad (3.8)$$

where the superscript indicates the iterate number and s^k is a positive scalar. By monitoring the convergence of a few of the branch circulations during the Gauss-Seidel iteration, we were always able to find a solution. In most cases, the loop circulations would eventually converge as well (that is, s^k would tend towards zero) but this usually

required a large number of iterations.)

If a good initial guess is available, then the number of Gauss-Seidel iterations is substantially reduced. In the case of attached flow, a good initial guess can come from another angle of attack while in the case of separated flow, the set of loop circulations from the previous wake iteration provides a good one as well. Frequently the number of iterations was large enough as to make Gauss-elimination the preferred scheme.

Control point location influences the structure of [A] and the resulting loads as well. Use of average control points does not necessarily result in [A] being strictly diagonally dominant. Nonetheless, the diagonal elements are always greater in absolute value than any of the off-diagonal elements. However, for the long thin panels near the nose of the body, the diagonal elements can overwhelm the off-diagonal elements and this seems to make the matrix product [A][G] sensitive to small changes in [G]. Using optimal control points minimizes the diagonal elements in [A] while leaving the off-diagonal elements essentially the same. Numerical examples in Chapter Four illustrate the effect of control placement on the calculated loads.

Another source of ill-conditioning is abrupt changes in the lattice spacing. A nearly regularly spaced uniform lattice with gradual changes in panel size and aspect ratio is recommended for reliable and efficient solutions.

There are also computer resource limitations. If an iterative scheme is used, the coefficient matrix can be stored on a low-speed device (disk or tape) and blocks of rows retrieved when needed. If a direct method is used, however, the coefficient matrix is modified during the solution process. If the coefficient matrix cannot be stored in memory then successive rewrites of the matrix to a low-speed device are necessary. This is time consuming for a large system of equations and if pivoting is used, the penalties of having to retrieve the coefficient matrix in column and then row order are considerable. If memory limitations are severe then an iterative method should probably be used. However, many modern computer system employ virtual memory management and extremely large systems (4000 equations or more) can be stored in memory for the time necessary to obtain a solution of the linear equations. Then the memory can be dynamically returned to the operating system so that it is not dedicated to the program while other calculations are performed.

An ingenious scheme has been tested by James and Clark (1979) to help reduce the effort required to solve the linear equations. They exploited the predictable nature of an influence matrix by expressing the rows and columns of the matrix in terms of either a Fourier or a eigenvector series. They then solved a reduced set of equations in terms of the coefficients of the basis functions enabling them to write an approximate solution of the complete system of equations. Results for two-dimensional flow problems indicated that considerable savings for three-dimensional problems could possibly be achieved. However, the structure and approximation of the influence matrix is much more complicated in the latter case.

The choice of solution technique for the system of equations depends on whether a good initial guess is available, the conditioning of the system, and the size of the system. We vary our choice of technique depending on the circumstances.

3.7 Wake Iteration Schemes

Once the no-penetration condition on the body is satisfied, we position the wake segments so that they are force-free. Since the influence of each wake segment is felt everywhere, moving any of the wake segments changes

the force-free position of all the other wake segments and results in the no-penetration condition being violated on the body. While this influence is minimal for those segments far away, the influence of segments nearby is substantial. Thus, the order of adjustment of the segments is important. We found that positioning the segments in turn resulted in faster convergence than positioning them all simultaneously for a fixed set of loop circulations. Typically, all the segments in the wake must be re-positioned three or four times before a reasonably force-free wake is obtained. In practice, the loads on the body are surprisingly insensitive to the wake position once the wake has begun to roll up.

The physics of the problem suggests judicious choices in the order of wake segment adjustment. If the flow is symmetric, we adjust corresponding pairs of segments on either side of the plane of symmetry simultaneously. Our experience has been that it is best to adjust the furthest upstream segments first as their position seems to converge rather quickly. We do not adjust the position of the segments in the last two or three wake lines. Their converged position is difficult to find and the effect on the region of interest is minimal. Evidently, the method tends to overestimate the distance the segments should be moved from one iterate to the next since relaxing the

predicted changes in the positions tends to stabilize the calculations and usually results in fewer iterations . In fact, relaxation factors as low as a tenth are not unreasonable. Especially in the early stages of the iteration when few numerical quantities are close to their converged values.

Our model of the wake corresponds to tracking the path of vorticity downstream with an Euler time integration scheme. Zorea and Rom (1978) used both an Euler method and a second-order Runge-Kutta method to solve for the wake position, but they did not comment on the differences they may have encountered between the two methods. Such a scheme would certainly take more computer time but would also be more stable than using the lower-order Euler method.

Finding a converged wake position with vortex-lattice methods sometimes requires several trial iterative schemes in combination with under-relaxing the wake motion. In fact, in solving for the separated flow over thin low aspect-ratio delta wings at moderate angles of attack, Mook (1980) observed that certain combinations of lattice parameters could induce a cyclic behaviour of wake position iterates after many iterations while the loop circulations had already converged. Moreover, averaging successive wake

iterates only caused a new set of cyclic wake iterates to develop. Under-relaxing the motion of the wake segments during the iteration process alleviated the problem.

Aparinov, Belotserkovskii, Nisht, and Solklova (1976) claimed that the failure of vortex-lattice methods to converge on a wake shape indicated vortex breakdown. This is improbable since so many parameters in the method influence the sequence of iterates. Moreover, for some problems, one combination of iteration parameters may induce convergence while another, equally plausible combination, may not.

3.8 Calculation of Loads

We use the steady Bernoulii equation to calculate the loads on the body:

$$C_p = \frac{P_\infty - P}{\frac{1}{2}\rho V_\infty^2} = 1 - \frac{V^2}{V_\infty^2} \qquad (3.9)$$

where P_∞ is the freestream dynamic pressure,

P is the local pressure,

V_∞ is the undisturbed freestream velocity,

ρ is the fluid density,

and V is the surface velocity.

We calculate the pressure coefficient on the body at the control points. We define the local normal-force coefficient for a fixed axial location on the body as:

$$C_n = \frac{1}{r}\int_0^{2\pi} C_p \cos\theta \, d\theta \qquad (3.10)$$

where r is the radius of the body and θ is the circumferential angle measured from the windward meridian.

The total velocity on the bound-vortex sheet is the sum of the contributions due to the freestream, all of the vortex segments in the flow, and one-half the jump in velocity across the vortex sheet. We calculated this jump as :

$$\vec{V} = \frac{1}{2}\,\vec{n} \times \vec{w} \qquad (3.11)$$

where $\vec{n}$ is the unit normal to the sheet and $\vec{w}$ is the vorticity vector for the panel as defined in (3.1).

3.9 Summary

In this chapter, we have described the vortex-lattice model that replaces the continuous vortex-sheet model presented in Chapter Two and an iteration procedure. In the next chapter, we present numerical examples that illustrate many of the concepts introduced here.

Chapter Four

Numerical Examples

To demonstrate the vortex-lattice method, we treat the flow over an inclined ogive-cylinder with a nose length of three diameters. The circumferential angle and axial starting location of the separation line are assumed to be known.

In cases with attached flow we compare our results those of the XYZPF computer code described in Dawson and Dean (1972). The XYZPF code employs Hess and Smith's (1962) source-distribution method to calculate flows over nonlifting bodies. It is important to note that the same panel arrangement has been used in the calculations for both the vortex-lattice method (VLM) and the source-distribution method (SDM). All results of the VLM and the SDM citied are from calculations specifically performed for use in this report.

In cases with separated flow we compare our results with those of the concentrated vortex core and feeding sheet model of Bryson (1959) as reported by Jepps (1977). Jepps treated the separation line on the body as the locus

of crossflow plane stagnation points. He also fixed the circumferential separation angle as we do here.

We measure the circumferential angle from the windward meridian. The circumferential angle of the separation line we denote as ϕ and the angle of attack we denote as α . All of the cases considered here are symmetric so we show results for one half of the body only. We specify a lattice with 'n' panels on the nose in the axial direction and 'm' panels everywhere on the body in the circumferential direction as an 'n x m' lattice. These quantities are illustrated in Figure 4-1.

If necessary, we use a cosine circumferential spacing of the panels and adjust it so that the separation line location falls on a longitudinal line in the bound-vortex lattice. That is, the spacing in the circumferential direction is related to the difference in the cosines of equal increments of an angle. This provides a smooth variation in the size of adjacent panels. If possible, a uniform circumferential distribution of panels is used. The circumferential spacing is arranged to be symmetric about the midplane of the body.

For comparisons of results from different calculations and numerical with experimental results, quantities are rarely available at the common stations on the body. To circumvent this problem, we use bicubic splines to interpolate the results. We use the trapezoidal rule for integrating the pressures around the body to obtain the normal-force coefficient.

4.1 Attached Flow Results

We first examine the effect of using area-weighted branch circulations in the pressure calculation when the lattice has an irregularity in the axial spacing. In Figure 4-2 the planviews of two lattices are show. Lattice 'a' has uniform axial spacing over the entire length of the body while lattice 'b' has an sudden change in the axial spacing immediately aft of the ogive-cylinder junction. The lattices have the same number of elements in the circumferential direction and they are evenly distributed.

In Figure 4-3 the pressure coefficients calculated for the case of zero angle of attack for both lattices are plotted with the experimental results cited in Faulker, Hess, and Giesing (1964). Optimal control points were used in all the VLM results shown. The results obtained using equally-weighted circulations near the nose for the uniform

and nonuniform lattices were virtually identical and are not shown. As demonstrated by the figure, the use of area-weighted circulations significantly reduced the evidence of the lattice irregularity in the pressure distribution. The panels which join to form the nose of the body are triangular. Therefore, we expect to see differences in the results using the two circulation rules near the nose as the figure demonstrates. The use of equally-weighted circulations near the nose resulted in pressure coefficients closer to experimental values. Thus, the use of area-weighted circulations provided for less accurate results near the nose and at the same time their use provided for more accurate results near the lattice irregularity. This probably indicates that the pressure calculation for panels that border other panels of widely different shape requires special consideration. That is, the assumptions reguarding vorticity modelling used in deriving the pressure calculation scheme we employ are not valid when panels of widely different shapes are adjacent. We see virtually no difference among any of the variations used here from just aft of the nose to just forward of the junction because the panels do not vary drastically from one to the next.

In the figures that follow we make comparisons of the results obtained by the SDM, the VLM, and experimental evidence. All calculations were performed on the same computer with precisely the same panel arrangement, where indicated.

In Figure 4-4a, we compare the results of the SDM, the VLM using optimal control points, and experiments. As expected, the results calculated with the SDM method agree more favorably with the experimental data near the nose of the body than do the results of the VLM. The results of the two methods are indistinguishable on the cylindrical portion of the body.

The influence of the axial density of elements on the results of the VLM is shown in Figure 4-4b for the case of zero angle of attack. An increase in the axial density of the elements provided for better agreement with experimental data in the nose region. A similar comparison for the SDM showed no discernible difference. The results suggest that the VLM is somewhat more sensitive to axial density of elements than the SDM is. However, this sensitivity is not extreme.

The influence of circumferential panel density on the pressure coefficient for the case of zero angle of attack is shown in Figure 4-5a for the VLM and in Figure 4-5b for the SDM. Surprisingly, the results of the VLM using 4 circumferential panels are more accurate than those using 14 circumferential panels. This is because in the latter case the panels have become long and thin. The closer the panels are to being square the better the results tend to be due to the assumptions made in the development of the surface vorticity model. Using area-weighted circulations will not alleviate the problem because adjacent panels have approximately the same area. The SDM seems to show the reverse behaviour. However, the influence of circumferential panel density on the calculated results is markedly different when the body inclined to the flow as we illustrate below.

The data suggests that the results of the VLM using optimal control points and the results of the SDM are relatively insensitive to panel density for the case of zero angle of attack so long as the panels remain approximately square.

We now investigate the effect of control-point location on the results of the VLM for the case of zero angle of attack. In Figure 4-6, the pressure coefficient

calculated by the VLM using the two choices of control-point placement is shown. Here, the use of optimal control points significantly improved the accuracy of the calculated pressure near the nose. The influence of control-point location diminishes as we move back along the body because the location of the two control point choices grow closer together. The two control point locations are coincident on the cylindrical portion of the body since the panels there are rectangular in shape.

However influence of control point placement is entirely different when the body is inclined to the flow. Moreover, the influence varies with the axial station and circumferential panel density. In Figure 4-7, we show the results for the first four axial calculation stations for the case of 15 degrees angle of attack using the VLM with optimal control-point placement. We see that the influence of circumferential panel density is more pronounced than it was in the case of zero angle of attack. This influence diminishes as we move back along the body.

In Figure 4-8, we show the corresponding results using average control-point placement. The sensitivity to circumferential panel density is much less severe. The reason that the station axial locations are different in the two figures is that average and optimal control points

are located at different axial stations. Rather than introduce interpolation errors that might contaminate the comparison, we chose to present data at the stations used in the calculations.

The corresponding figure for the SDM is presented in Figure 4-9. The SDM shows very little sensitivity to circumferential panel density for this case.

In Figure 4-10, we show representative results for all three calculations interpolated to common axial stations for comparison. The difference between the results of the SDM and the VLM using optimal control points grow smaller as we move axially along the body while the results of the VLM using average and optimal control points grow more parallel. This is illustrated further in the next two figures.

We compare the results of the calculations with experimental values reported by Tinling and Allen (1962) in Figure 4-11. The experimental data were taken at Reynolds numbers of 440,000 and 3,000,000 based on the test model's length of ten diameters. At $x/d = 0.5$, the pressure distribution calculated with the vortex-lattice method using optimal control points agrees better with the experiments than the one calculated using average control points. The results of calculations using average control

points appear almost parallel to those using optimal control points and to the experimental results. The difference in the experimental results due to Reynolds number effects is greatest on the leeward side of the body - precisely where the results of the VLM also show the greatest variation from being parallel to one another. Except for the dip in the average control-point results, the difference between the two VLM calculations at this station represent approximately a constant shift in the pressure coefficient throughout the circumference of the section. Such a shift in the pressure coefficient will not influence the resultant normal-force coefficient since the integral of a constant over the circumference of a section vanishes. Subsequent boundary-layer calculations would remain largely unaffected since the pressure gradient is also unaffected by a constant shift in pressure,

At $x/d = 2$, the shift in the pressure distribution is smaller but still present. Also, the results of the VLM using optimal control points appear to be slightly larger than the experimental results. The results using average control points now even appear to be slightly more accurate but this is probably fortuitous. There also seems to be more of a Reynolds number effect at this station.

In both figures, the results of the SDM agree as well as the results of the VLM using optimal control points.

Figure 4-12 displays the normal-force coefficient vs. axial distance for three different angles of attack. In all three cases, results of the VLM using average control points agree better than those of the VLM using optimal control points, even though the opposite behaviour was experienced when viewing pressure distribution comparisons. The reason for the behaviour is not obvious. As expected the shift in the the pressure distribution due to control-point placement did not substantially alter the normal-force coefficient for the stations we examined. Unfortunately experimental data was unavailable for intermediate stations. The results of the SDM are reasonable for all three cases.

The normal-force coefficient on the afterbody is zero for attached flow because there is no lift mechanism present. The experimental data indicates that lift is present aft of the ogive-cylinder junction since the flow begins to separate from the body there.

The variation of the experimental data with Reynolds number indicates that viscous effects are of some importance. Including the displacement thickness of the boundary layer in the dimensions of the body might improve

agreement between calculated and measured results.

4.2 Separated Flow Results

We now compare results of the VLM in cases with separated flow to the calculations of Jepps (1977) and the experimental results of Tinling and Allen (1962). We adjust the separation angle such that the location of the control point just below (that is, just windward) of the separation line is approximately the same in our calculations as it was in Jepps'. Since we used a circumferential spacing which was far coarser than Jepps', our separation angle is somewhat higher than Jepps'. That is, the separation angle in the present calculations is located more towards the leeward side of the body. We chose Jepps' work as representative of two-dimensional analogy based methods.

In Figure 4-13, the wake off one side of the body is shown for 10, 15, and 20 degrees angle of attack. The figure is a computer generated drawing of the actual calculated solutions calculated by the present method. The separation angle for all cases is 140 degrees. There are 24 wake lines with the first line having 30 finite vortex segments and each subsequent line having one segment fewer than the line in front of it. This allows for many of the

wake lines to end at approximately the same axial location.

Figure 4-14 shows the front view of the same wakes. In the figure all the wake lines have been collapsed onto the viewing plane. The diagram does not represent a section view of the wake but rather all the wake lines are shown together as they would be seen by an observer in front of the body looking ft. While most of the lines roll up in a more or less organized vortex core, a few of the lines extend beyond the core envelope. These lines originate near the end of the body. It proved to be very time consuming to find their converged position while at the same time their influence on the loads in the region of interest on the body was minimal. For the sake of economy in the examples shown, the last three wake lines were not adjusted to a force-free position and thus the few lines preceding them converged to unrealistic shapes. The influence on the loads on the body in the region of interest was still negligible.

To demonstrate the behaviour of the circumferential pressure distribution at different axial stations in the attached to the separated flow region we compare the calculated attached and separated circumferential pressure distributions for several consecutive axial calculation stations in Figures 15 and 16. The figure illustrates

circumferential and longitudinal changes in the pressure distribution as we move from attached to separated regions on the body.

The first vortex line is attached to the body between stations 12 and 13. Only a few stations later, the shape of the circumferential pressure distribution does not change from one station to the next. The presence of the separated vortex sheet increases the pressure in the front of the separation line over the value it had for attached flow while the pressure behind the separation line falls below the value for attached flow. Since there are only two circumferential panels behind the separation line, the calculations do not reproduce flow details there.

Figures 4-17 through 4-22 display the various circumferential pressure distributions for 10, 15, and 20 degrees angle of attack for $x/d = 4.5$, 6, and 7.5. In all cases the cross-flow analogy method of Jepps overpredicted the rise in the pressure in front of the separation line and the results show a sharper drop in the pressure behind the separation line than do those of the present method. Neither method does well behind the separation line. Both method's results are least accurate at the higher angles of attack. We note that the Reynolds number effect on the experimental data is more pronounced at higher angles of

attack.

Figures 4-23 and 4-24 display the normal-force coefficient vs. axial distance for different separation line locations and angles of attack. Both the cross-flow analogy and vortex-lattice method calculated forces which level off on the afterbody quickly at 10 degrees angle of attack but not at all for 20 degrees angle of attack. The sharp peaks in the results for the vortex-lattice method are present because of the sudden departure in the lattice configuration there due to the presence of the free-vortex sheet. The bound-vortex lattice for these examples was tested to ensure that no irregularities in the results were due to irregularities in the bound-vortex lattice spacing. Jepps mentioned also that his method produced unreliable results in this region of the body and he smoothed the normal-force coefficient using values from neighboring stations to make the results look more realistic. We have done no such smoothing here. Once again, Reynolds number effects are more significant at the the higher angles of attack.

The results for the two separation angles used are shown in Figure 4-25 for the case of 15 degrees angle of attack. It is interesting that the change in separation line location caused approximately a constant shift in the

normal-force coefficient on the lifting portion of the body. A shift in the separation line circumferential angle, then, has a similar effect on the loads as a change in the Reynolds number.

Figure 4-26 shows the normal-force coefficient vs. axial distance along the body for each iteration of the loop circulations. After only three iterations the normal-force coefficient has almost converged.

We plotted the loop circulation strength vs. circumferential angle for stations 5 and 25 in Figure 4-27. Station 5 is located on the nose of the body and the flow is fully attached. Station 25 is located on the afterbody and separation is present there. The shape of the curves is similar in both cases in the attached region of the body. That is, the windward side of the body experiences a similar change in the loop circulation strength as we move circumferentially around the body. Since the branch circulations (and hence the velocity field) are dependent on the shape of the curve, we could fix the loop circulations in that attached flow regions of the body and calculate only those loop circulations which are significantly affected by the presence of the separated wakes. This would dramatically reduce the computer time needed for a solution. This would cause an error in the

branch circulations of the segments which border an opening on the body surface but typically the only opening is perhaps an open tail and that would have a minimal effect of the upstream portion of the flow field.

Chapter Five

Conclusions and Recommendations

We developed a nonlinear vortex-lattice method to treat the steady flow over prolate bodies with open separation moving through an inviscid incompressible fluid. The strength and position of the body wake is found as part of the solution. Specifically, flows with smooth-surface separation have been considered as opposed to flows with sharp-edge separation treated with vortex-lattice methods in the past.

From our comparisons, we can conclude that the vortex-lattice method is more sensitive to lattice arrangement than the source-distribution method of Hess and Smith. We found that use of area-weighted circulations significantly reduced the effect of lattice irregularities in the calculated results. Use of optimal control points with the vortex-lattice method led to improved results for the zero angle of attack case and worse results when the body was at incidence. Moreover, using optimal control points made the results more sensitive to lattice design. Also, we found that if the panels become long and thin in

one direction, the accuracy of the results can be degraded even though a denser lattice arrangement was being used.

In the case of separated flow, we found that both the vortex-lattice method and the two-dimensional cross-analogy Bryson (1959) as applied by Jepps (1977) overpredict the pressure in front of a separation line and underpredict the pressure behind a separation line. Neither method predicts accurate loads near the beginning of a separation line.

While we only considered steady symmetric flows, vortex-lattice methods are applicable to asymmetric unsteady flows as well. However, an unsteady separation line would be necessary. The motion of a separation line on a body during an unsteady maneuver may be difficult to model.

The general trend of the results strongly indicate that the accurate use of the vortex-lattice method requires great care in the choice of lattice parameters - particularly in the areas of in panel arrangement and control point placement.

For immediate areas of study we recommend the following :

1. Modification of the lattice to allow the free-vortex sheet to leave the body tangentially.
2. Exploration of means to reduce the deviations in the

pressures near the beginning of a free-vortex sheet and behind it.

3. Investigation of paneling techniques that allow for the separation line angle to vary along the body.

4. Coupling of the method with a boundary-layer scheme to solve for the location of the separation lines on the body via a viscous-inviscid calculation procedure.

References

Allen, H.J. and E.W. Perkins, 1951. "A Study of Effects of Viscosity on Flow over Slender Inclined Bodies of Revolution," NACA Report 1048.

Angelucci, S.B., 1971. "A Multivortex Method for Axi-symmetric Bodies at Angle of Attack," Journal of Aircraft, Vol. 8, No. 12, pp. 959-966, December.

Aparinov, V.A., S.M. Belotsekovskii, M.I. Nisht, and O.N. Sokolva, 1976. "On the Mathematical Simulation in an Ideal Fluid of Separated Flow Past a Wing and the Destruction of the Vortex Sheet," Dokl. Ak. Nauk. SSSR Vol. 227, pp. 820-823, Translation as Sov. Phy. Dokl., Vol. 21, No. 4, pp. 181-183.

Asfar, K.R., 1978. "Application of the Vortex-Lattice Technique to Arbitrary Bodies," M.S. Thesis, Department of Engineering Science and Mechanics, Virginia Polytechnic Institute and State University, Blacksburg, Virginia.

Asfar, K.R., D.T. Mook, and A.H. Nayfeh, 1978. "Application of the Vortex-Lattice Technique to Arbitrary Bodies," AIAA Paper No. 78-1205. Also in Journal of Aircraft, Vol. 16, No. 7,July, 1979, pp. 421-4.

Atta, E.H., O.A. Kandil, D.T. Mook, and A.H. Nayfeh, 1976. "Unsteady Flow Past Wings Having Sharp-Edge Separation," NASA SP-405, (Vortex-Lattice Utilization Workshop), pp. 407-418.

Atta, E.H. and A.H. Nayfeh, 1978. "Nonlinear Aerodynamics of Wing-Body Combinations," AIAA Paper No. 78-1206.

Baker, G.R., 1980. "A Test of the Method of Fink and Soh for Following Vortex sheet Motion," Journal of Fluid Mechanics, Vol. 100, Part 1, pp. 209-20.

Belotserkovskii, S.M., 1966. "Gust Effects on Wings of Complex Planforms at Subsonic Speeds," Mekanika Zhrdkosti I Craza, Vol. 4, pp. 129-138.

References (cont'd)

Birkhoff, G.D. amd J. Fisher, 1959. "Do vortex sheets roll up?", Rc. Circ. mat. Palermo Ser., Vol. 8, No. 2, pp. 77-90.

Bryson, A.E., 1959. "Symmetric Vortex Separation on Circular Cylinders and Cones," Journal of Applied Mechanics, Vol. 26, pp. 643-648, December.

Chang, M.S. and P.C. Pien, 1975. "Hydrodynamic Forces on a Body Moving Beneath a Free Surface," Proceedings, First International Conference on Numerical Ship Hydrodynamics, David W. Taylor Naval Ship Research and Development Center, Bethesda, Maryland, pp. 539-59.

Chow, S.K, A.Y. Hou, and L. Landweber, 1976. "Hydrodynamic Forces and Moments Acting on a Body Emerging from an Infinite Plane," The Physics of Fluids, Vol. 19, pp. 1439-1449.

Chow, S.K., Y.T. Lee, and E.A. Owen, 1982. "A Integral-Equation Singularity Method Approach for Three-Dimensional Electromagnetic Field Determination in the End Region of a Turbine Generator," IEEE Transactions on Magnetics, Vol. MAG-18, No. 2, March.

Davey, A., 1961. "Boundary-Layer Flow at a Saddle Point of Attachment," Journal of Fluid Mechanics, Vol. 10, pp. 593-610.

Dawson, C.W. and J.S. Dean, 1972. "The XYZ Potential Flow Program," DTNSRDC Report 3892, June.

Eichelbrenner, E.A., 1955. "Observations on a Criterion for Three-Dimensional Laminar Boundary-Layer Separation," Rech. Aéron., No. 40, pp. 3-5; also NRC (Canada) TT-962, 1961.

Eichelbrenner, E.A. and A. Oudart, 1955. "Three-Dimensional Laminar Boundary-Layer Separation," Rech. Aéron., No. 47, pp. 11-4; also NRC (Canada) TT-963, 1961.

References (cont'd)

Faulkner, S., J.L. Hess, and J.P. Giesing, 1964. "Comparsion of Experimental Pressure Distributions with Those Calculated by the Douglas-Neumann Program," Douglas Aircraft Company, Report No. LB31831, December.

Fiddes, S.P., 1980. "A Theory for the Separated Flow Past a Slender Elliptic Cone at Incidence," RAE Tech Memo 1858.

Fidler, J.E. and M.C. Bateman, 1975. "Asymmetric Vortex Effects on Missile Configurations," AIAA Paper No. 75-209, January.

Fink, P.T. and W.K. Soh, 1974. "Calculations of Vortex Sheets in Unsteady Flow and Applications in Ship Hydrodynamics," Proceedings of the 10th Symposium on Naval Hydrodynamics, U.S. Office of Naval Research, pp. 464-489.

Gerrard, J.H., 1967. "Numerical Computation of the Magnitude and Frequency of the Lift on a Circular Cylinder," Phil. Transactions Royal Society, Vol. 261, No. 1118, pp. 137-62.

Gersten, K., 1961. "Nichlineare Tragflachenthecrie insbesondere für Tragflachen mit kleinem Seitenverheltnis," Ing.-Arch. Bd., Vol. 30, pp. 431-52.

Goult, R.J., R.F. Hoskins, J.A. Milner, M.J. Pratt, 1974. Computational Methods in Linear Algebra. John Wiley & Sons, New York.

Hama, F.R. and E.R. Burke, 1960. "On the Rolling up of a Vortex Sheet," Univerisity of Maryland, TN No. BN-220.

Hess, J.L. and A.M.O. Smith, 1962. "Calculation of Nonlifting Potential Flow about Arbitrary Three-Dimensional Bodies," Douglas Aircraft Company, Report No. ES-40622, March.

References (cont'd)

Hess, J.L. and A.M.O. Smith, 1964. "Calculation of Nonlifting Potential Flow about Arbitrary Three-Dimensional Bodies," Journal of Ship Research, Vol. 8, September.

Hess, J.L. and A.M.O. Smith, 1966. "Calculation of Nonlifting Potential Flow about Arbitrary Three-Dimensional Bodies," Progress in Aeronautical Sciences, Vol. 8 Pregammon Press, New York. Also as Douglas Aircraft Company Engineering Paper 3327.

Hunt, J.C.R., C.J. Abell, J.A. Peterka, and H. Woo, 1978. "Kinematical Studies of the Flows Around Free or Surface-Mounted Obstacles; Applying Topology to Flow Visualization," Journal of Fluid Mechanics, Vol. 86, pp. 179-200.

James, R.M. and R.W. Clark, 1979. "A New Approach to the Solution of Large, Full-Matrix Equations - A Two-Dimensional Potential Flow Feasibility Study," NASA CR-3173.

Jepps, S.A., 1977. "A Theoretical Investigation of the Subsonic Flow Past an Ogive-Cylinder Body," British Aircraft Corporation, Math Services Notes 226, March.

Johnson, F.T. and P.E. Rubbert, 1975. "Advanced Panel-Type Influence Coefficient Methods Applied to Subsonic Flows," AIAA Paper No. 75-50.

Johnson, L. and R.D. Riess, 1977. Numerical Analysis, Addison-Wesley Publishing Company, Reading, Mass.

Jordan, S.K. and J.E. Fromm, 1972. "Oscillatory Drag, Lift, and Torque on a Circular Cylinder in Uniform Flow," Vol. 15, No. 3, pp. 371-6.

References (cont'd)

Kandil, O.A., 1974. "Prediction of the Steady Aerodynamic Loads on Lifting Surfaces Having Separation on Sharp Edges," Ph.D. Disseration, Department of Engineering Science and Mechanics, Virginia Polytechnic Institute and State University, Blacksburg, Virginia.

Kandil, O.A., L-C. Chu, and E.C. Yates Jr., 1980. "Hybrid Vortex Method for Lifting Surfaces with Free-Vortex Flow," AIAA Paper No. 80-0070, presented at the 18th AIAA Aerospace Sciences Meeting, January 14-16, Pasadena, California.

Kandil, O.A., D.T. Mook, and A.H. Nayfeh, 1976. "A New Convergence Criterion for the Vortex-Lattice Models of Leading-Edge and Wing-Tip Separation," NASA SP-405 (Vortex-Lattice Utilization Workshop), pp. 285-300.

Kao, H.C., 1975. "Side Forces on Unyawed Slender Inclined Aerodynamic Bodies," Journal of Aircraft,Vol. 12, No. 3, March, pp. 142-50.

Karamcheti, K., 1966. Principles of Ideal-Fluid Aerodynamics, John Wiley and Sons, New York.

Kármán, T. von, 1930. Calculation of Pressure Distribution on Airship Hulls," NACA Tech Memo No. 574.

Kellogg, O.D., 1929. Foundations of Potential Theory, Dover Publications, New York, pp. 1-138.

Kelly, S.G., 1977. "A Systematic Investigation of the Parameters Affecting the Accuracy of the Vortex-Lattice Method," M.S. Thesis, Department of Engineering Science and Mechanics, Virginia Polytechnic Institute and State University, Blacksburg, Virginia.

Kubin, J.S., 1973. "An Analysis of Steady Asymmetric Vortex Shedding from a Missile at High Angles of Attack," M.S. Thesis, Air Force Institute of Technology, November.

References (cont'd)

Laird, A.D.K., 1971. "Eddy Formation Behind Circular Cylinders," Proceedings, American Civil Engineering Journal, Hyd. Div. HY6, pp. 763-75.

Landweber, L., 1974. Discussion of paper by Wu and Chwang (1974) 10th Symposium of Naval Hydrodynamics, MIT, June.

Landweber, L. and Macagno, M., 1969. "Irrotational Flow About Ship Forms," Institue Hydraulic Research Report No. 123, The University of Iowa, Iowa City, Iowa.

Legendre, R., 1956. "Séparation de l'Écoulement Laminaire Tridimensionnel," La Recherche Aéronautique, no. 54, pp. 3-8.

Legendre, R., 1965. "Lignes de Courant d'un Écoulement Continu," Recherche Ae'rospatiale, No. 105, pp. 3-9.

Legendre, R., 1972. "La Condition de Joukowshi en Écoulement Tridimensionnel," Recherche Aérospatiale, Vol. 5, pp. 241-8.

Legendre, R., 1977. "Lignes de Courant d'un Écoulement Permanent: Découllement et Séparation," Recherche Aérospatiale, Vol. 6, pp. 327-55.

Levin, D. and J. Katz, 1980. "A Vortex-Lattice Method for the Calculation of the Nonsteady Separated Flow over Delta Wings," AIAA Paper No. 80-1803.

Lighthill, M.J., 1963. "Attachment and Separation in Three-Dimensional Flow," Laminar Boundary Layers, edited by L. Rosenhead, Oxford University, pp. 72-82.

Marshall, F.J. and F.D. Deffenbaugh, 1974. "Separated Flow over Bodies of Revolution using an Unsteady Discrete-Vorticity Cross Wake: Part I, Theory and Application," NASA CR-2414, June.

Maskell, E.C., 1955. "Flow Separation in Three Dimensions," RAE Aero Report 2565.

References (cont'd)

Maskew, B., 1981. "Prediction of Subsonic Aerodynamic Characteristics - A Case for Low-Order Panel Methods," AIAA Paper No. 81-0252, presented at the 19th AIAA Aerospace Sciences Meeting, January 12-15, St. Louis, Missouri.

Maskew, B., B.M. Rao, and F.A. Dvorak, 1980. "Prediction of Aerodynamic Characteristics for Wings with Extensive Separations," AGARD CP-291-31.

Mook, D.T., 1980. Private Communication.

Mook, D.T. and S.A. Maddox, 1974. "Extension of a Vortex-Lattice Method to Include the Effects of Leading-Edge Separation," Journal of Aircraft, Vol. 11, No.2, p. 127.

Nikolitsch, D., 1978. "Normal Force and Pitching Moment Coefficients of Wing-Body Combinations at Very High Angles of Attack," AIAA Paper No. 78-63.

Noblesse, F., 1983. "A Slender-Ship Theory of Wave Resistance," Journal of Ship Research, Vol. 27, No. 1, March, pp. 13-33.

Noblesse, F. and G. Triantafyllou, 1983. "Explicit Approximations for Calculating Potential Flow about a Body," Journal of Ship Research, Vol. 27, No. 1, March, pp. 1-12.

Oswatitsch, K., 1957. "Die Ablösungsbedingung von Grezschichten," Grenzschichtforschung, edited by H. Görtler, IUTAM Symposisum Freiburg, Springer-Berlin. Also in a translation by A.Kluwick, 1980. "The Conditions for the Separation of Boundary Layers," Contributions to the Development of Gasdynamics, edited by W. Schneider and M. Platzer, F. Vieweg and Sohn,Braunschweig, West Germany.

Peake, D.J. and M. Tobak, 1980. "Three-Dimensional Interactions and Vortical Flows with Emphasis on High Speeds," AGARDograph No. 252, July. Also NASA TM-81169, March, 1980.

References (cont'd)

Perry, A.E. and B.D. Fairlie, 1974. "Critical Points in Flow Patterns," Advances in Geophysics, Vol. 18b, Academic Press, New York, pp. 299-315.

Pien, P.C., 1964. "The Application of Wavemaking Resistance Theory to the Design of Ship Hulls with Lower Total Resistance," Presented at the 5th Symposisum of Naval Hydrodynamics, Bergen, Norway.

Poincaré, H., 1928. "Oeuvres de Henri Poincaré, Tome 1," Gauthier-Villars et Cie, Paris.

Rehbach, C., 1977. "Numerical Investigation of Vortex Sheets Issuing from a Separation Line Near the Leading Edge," NASA TM-F 15, 330.

Rosenhead, L., 1932. "Formation of Vorticies from a Surface of Discontinuity," Proc. Roy. Soc. A, Vol. 134, pp. 170-92.

Sarpkaya, T., 1966. "Separated Flow about Lifting Bodies and Impulsive Flow about Cylinders," AIAA Journal, Vol. 4, pp. 414-20.

Sarpkaya, T., 1968. "An Analytical Study of Separated Flow about Circular Cylinders," Transactions ASME Journal, Basic Engineering, Vol. 90, pp. 511-20.

Sarpkaya, T. and R.L. Schoaff, 1979. "Inviscid Model of Two-Dimensional Vortex Shedding of a Circular Cylinder," AIAA Journal, Vol. 17, No. 11, pp. 1193-1200.

Schindel, L., 1965. "Effect of Vortex Separation on Lifting Bodies of Elliptic Cross-Section," MIT Tech Report 118, September.

Schindel, L., 1969. "Effect of Vortex Separation on Lift Distribution of Elliptic Cross-Section," Journal of Aircraft, Vol. 6, No. 6, November-December, pp. 537-43.

References (cont'd)

Schoaff, R.L., 1978. "A Discrete Vortex Analysis of Flow about Stationary and Transversely Oscillating Circular Cylinders," Ph.D. Disseration, Naval Postgraduate School, Monterey, California.

Schroder, W., 1978. "Berecnug der Nichtlinearen Beiwerte von Flugeln mit Kleinem und mittlerem Seitenverhlatnix nach dem Wirbelleiterverfahren in inkompressbiler Stromung," DFVLR-FB-78-26. Translated as ESA-TT-585.

Sears, W. R., 1948. "The Boundary Layer on Yawed Cylinders," Journal of Aeronautical Sciences, Vol. 15, No. 1, January, pp. 49-52. Also in Collected Papers of W.R. Sears through 1973, N.H. Kemp, editor, Valley Offset, New York.

Sheffield, J.S. and F.D. Deffenbaugh, 1980. "A Three Dimensional Vortex Wake Model for Missiles at High Angles of Attack," NASA CR-3208.

Smith, F.T., 1978. "Three-Dimensional Viscous and Inviscid Separation of a Vortex Sheet from a Smooth Nonslender Body," RAE Technical Report 78095.

Smith, J.H.B., 1969. "Remarks on the Structure of Concial Flow," RAE Technical Report 69119.

Smith, J.H.B., 1975. "A Review of Separation in Steady Three-Dimensional Flow," AGARD CP-168, Paper 31.

Smith, J.H.B., 1977. "Behaviour of a Vortex Sheet Separating from a Smooth Surface," RAE Techincal Report 77058, April.

Smith, J.H.B., 1978. "Inviscid Fluid Models for Three-Dimensional Separation at High Reynolds Numbers," AGARD LS-94.

Smith, J.H.B., 1980. "Vortical Flows and Their Computation," Part of the von Karman Institute for Fluid Dynamics Lectures Series in Computational Fluid Dynamics, March.

References (cont'd)

Sychev, V.V., 1972. "On Laminar Separation," Izv. Akad. Nauk. Mekh. Zhid. Gaza, No. 3, pp. 47-50. Translated in Fluid Dynamics, Plenum, March/April, 1974, pp. 407-417.

Thoman, D.C. amd A.A. Szewczyk, 1969. "Time Dependent Viscous Flow over a Circular Cylinder," Physics of Fluids, Suppl. II, pp.76-86.

Thompson, K.S. and D.F. Morrison, 1971. "The Spacing, Position, and Strength of Vorticies in the Wake of Slender Cylindrical Bodies at Large Incidence," Journal of Fluid Mechanics, Vol. 50, Part 4, December, pp. 751-83.

Tinling, B.E. and C.W. Allen, 1962. "An Investigation for the Normal-force and Vortex-Wake Characteristics of an Ogive-Cylinder Body at Subsonic Speeds," NASA TN D-1297, April.

Tobak, M. and D.J. Peake, 1981a. "Topology of Three-Dimensional Separated Flows," NASA TM-81294. Also published in Annual Review of Fluid Mechanics, Vol. 14, 1982.

Tobak. M. and D.J. Peake, 1981b. "Topological Structure of Three-Dimensional Separated Flows," AIAA Paper No. 81-1200, presented at the AIAA 14th Fluid and Plasma Dynamics Conference, June 23-25, Palo Alto, California.

Uchiyama, N., R.P. Mikkilineni, and J.M. Wu, 1978. "The Analysis of Wing-Body Combinations at Moderate Angles of Attack," AIAA Paper No. 78-62, presented at the AIAA 16th Aerospace Sciences Meeting, January 18-18, Huntsville, Alabama.

Walitt,L. and J.G. Trulio, 1971. "A Numerical Method for Computing Three-Dimensional Viscous Supersonic Flow Fields about Slender Bodies," NASA CR-1963, November.

Wardlaw, A.B., 1973. "Prediction of Normal Force, Pitching Moment, and Yawing Force on Bodies of Revolution at Angles of Attack up to 50 degrees using a Concentrated Vortex Flow Field Model," NOL TR 73-209, October.

References (cont'd)

Wardlaw, A.B., 1975. "Multivortex Model of Asymmetric Shedding on Slender Bodies at High Angle of Attack," AIAA Paper No. 75-123, January.

Webster, W.C., 1975. "The Flow about Arbitrary, Three-Dimensional Smooth Bodies," Journal of Ship Research, Vol. 19, No. 4, pp. 206-218.

Wu, T.Y. and A.T. Chwang, 1974. "Double Body Flow Theory - A New Look at the Classical Problem, Presented at the 10th Symposium Naval Hydrodynamics, MIT, June.

Yanta, W.J. and A.B. Wardlaw, Jr., 1982. "The Secondary Separation Region on a Body at High Angles of Attack," AIAA Paper No. 82-0343.

Yen, A., D.T. Mook, and A.H. Nayfeh, 1981. "A Continuous-Vorticity Panel Method for Lifting Surfaces," AIAA Paper No. 81-1895, presented at the AIAA Atmospheric Flight Mechanics Conference, August 19-21, Albuquerque, New Mexico.

Zorea, C.R. and J. Rom, 1978. "The Calculation of Non-Linear Aerodynamic Charactersitics of Wings and their Wakes in Subsonic Flow," Israel Journal of Technology, Vol. 16, pp. 83-96.

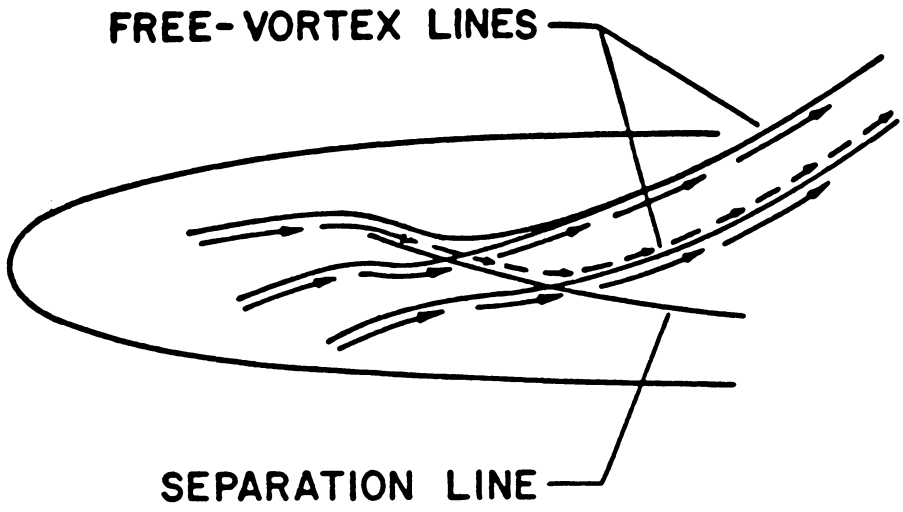

OPEN SEPARATION

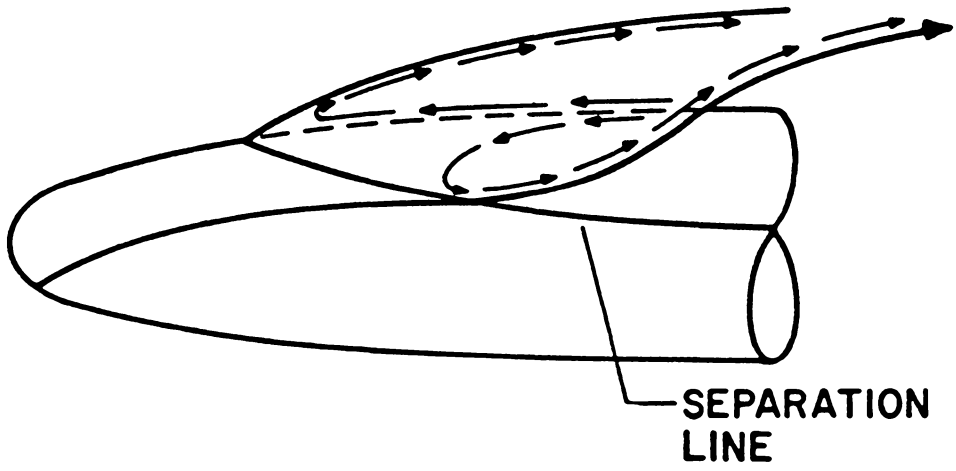

CLOSED SEPARATION

Figure 1-1 Schematic views of open and closed separation patterns.

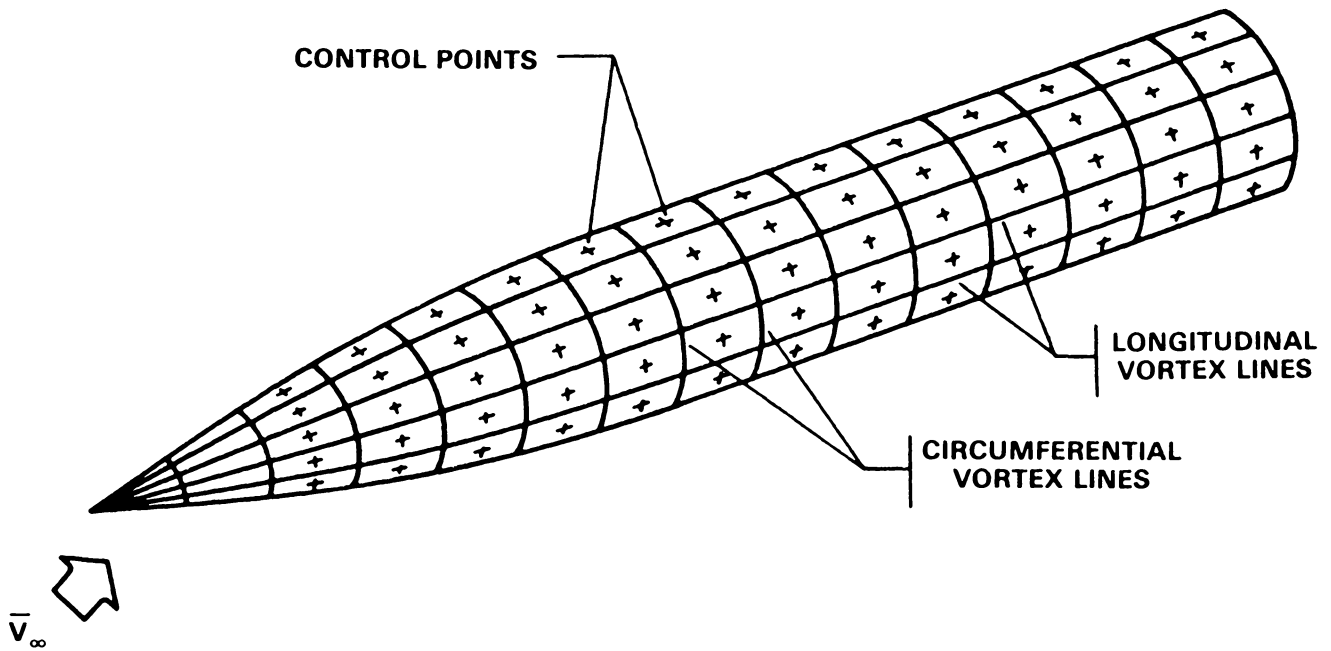

Figure 3-1 Schematic view of a bound-vortex lattice.

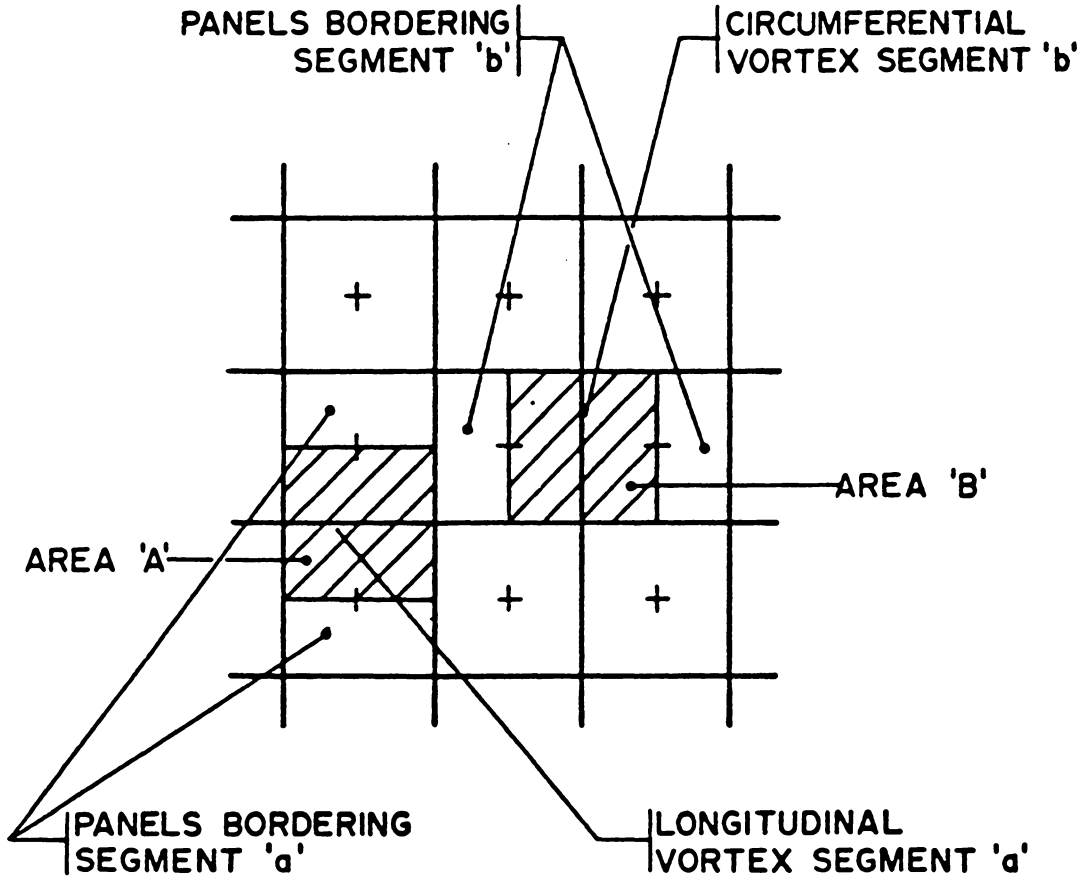

Figure 3-2 Representation of surface vorticity by bound-vortex segments.

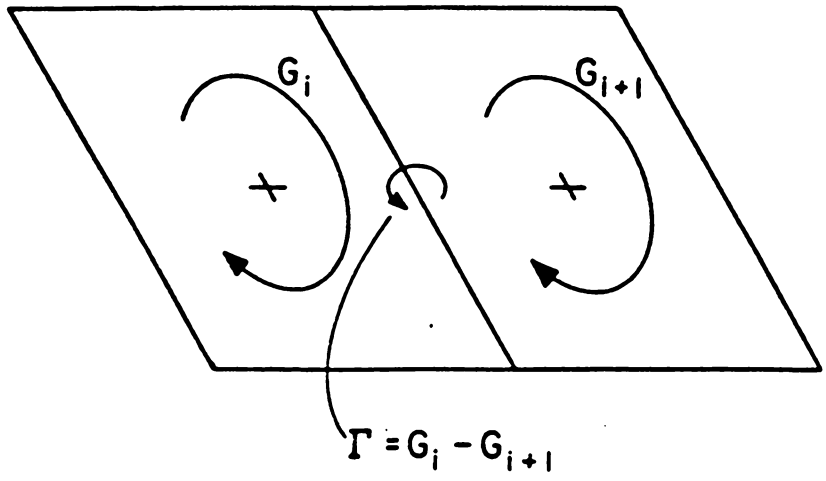

Figure 3-3 Definition of loop and branch circulations.

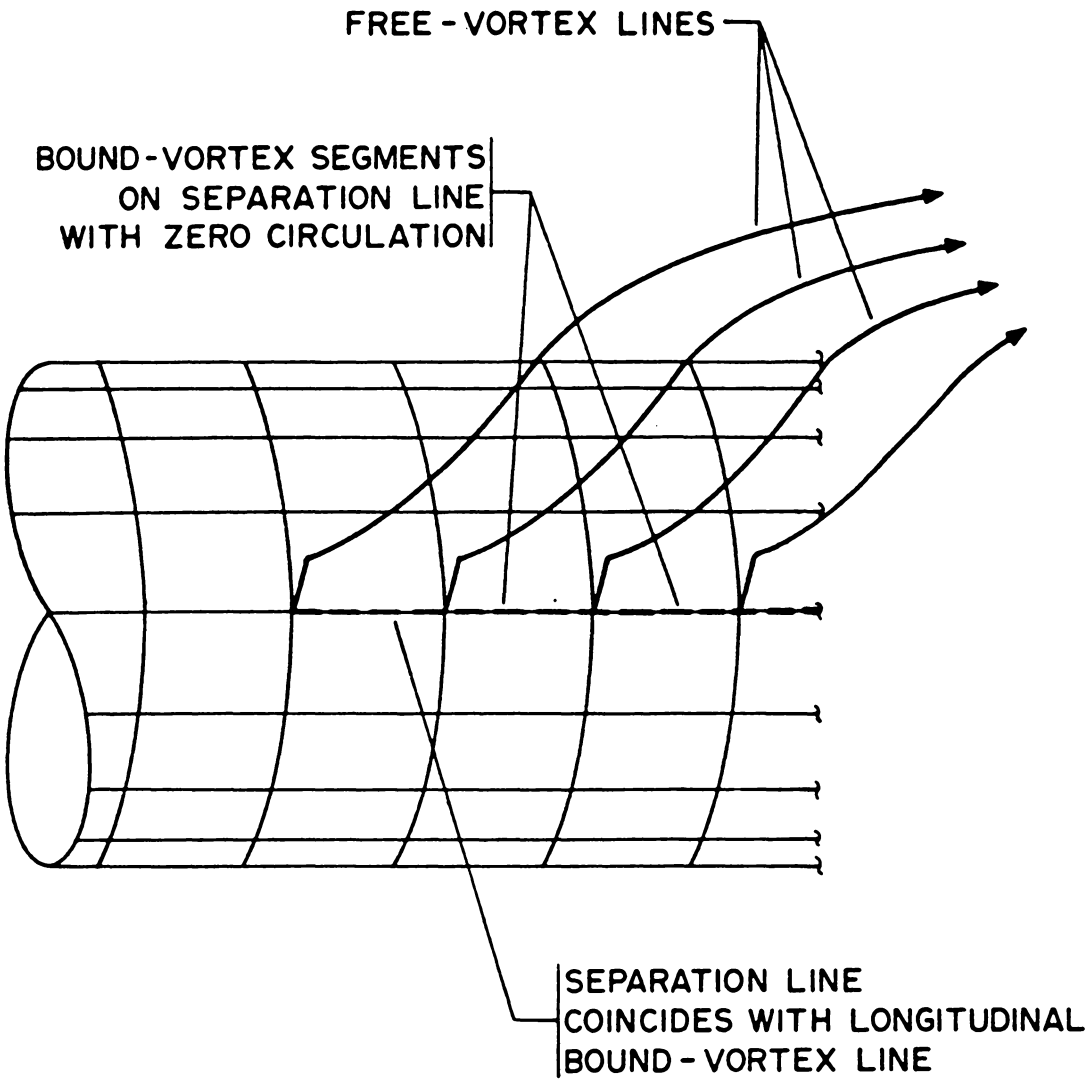

Figure 3-4 Schematic view of the attachment of a free- and bound-vortex lattice.

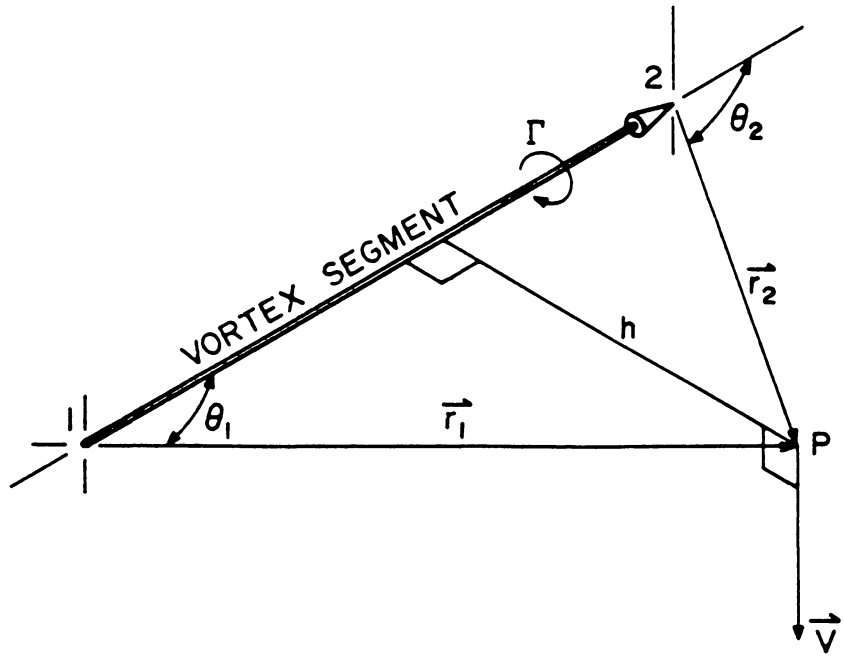

Figure 3-5 Definition of quantities used in the Biot-Savart law.

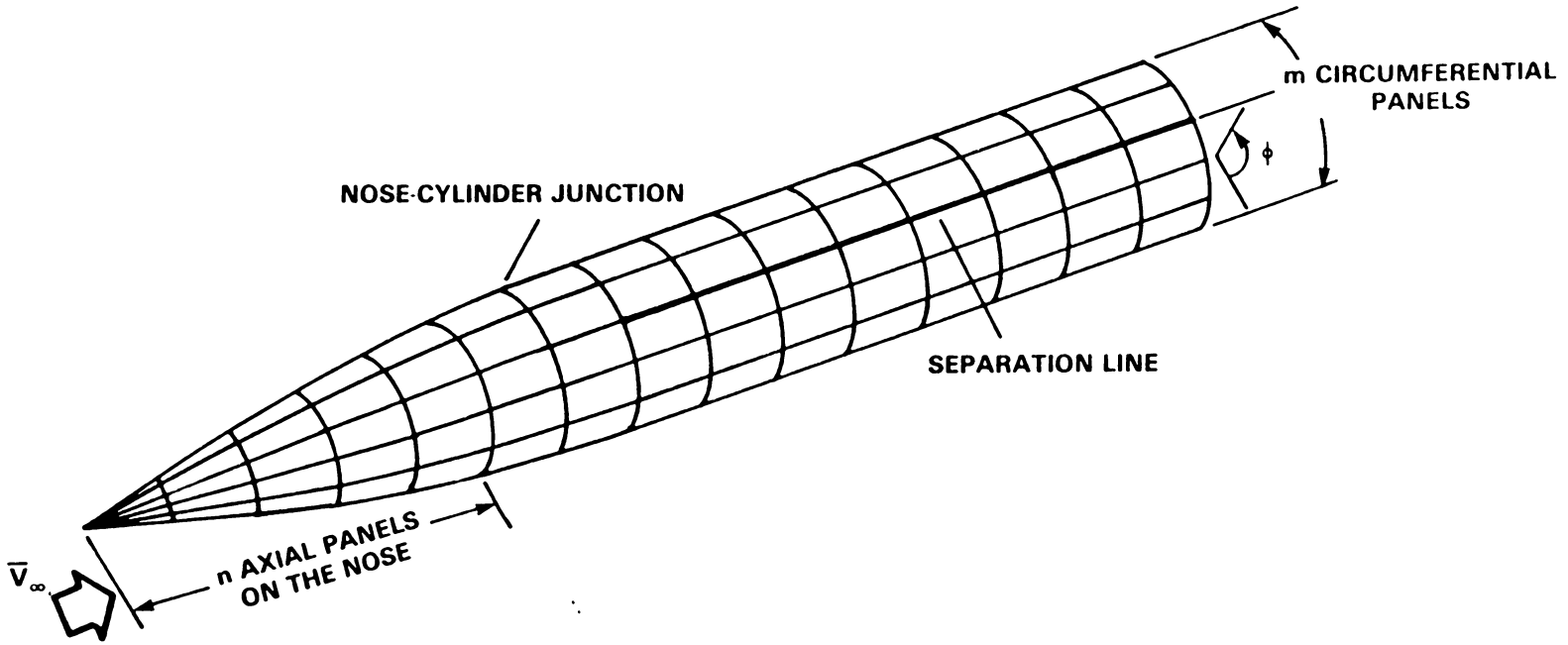

Figure 4-1 Definition of lattice quantities.

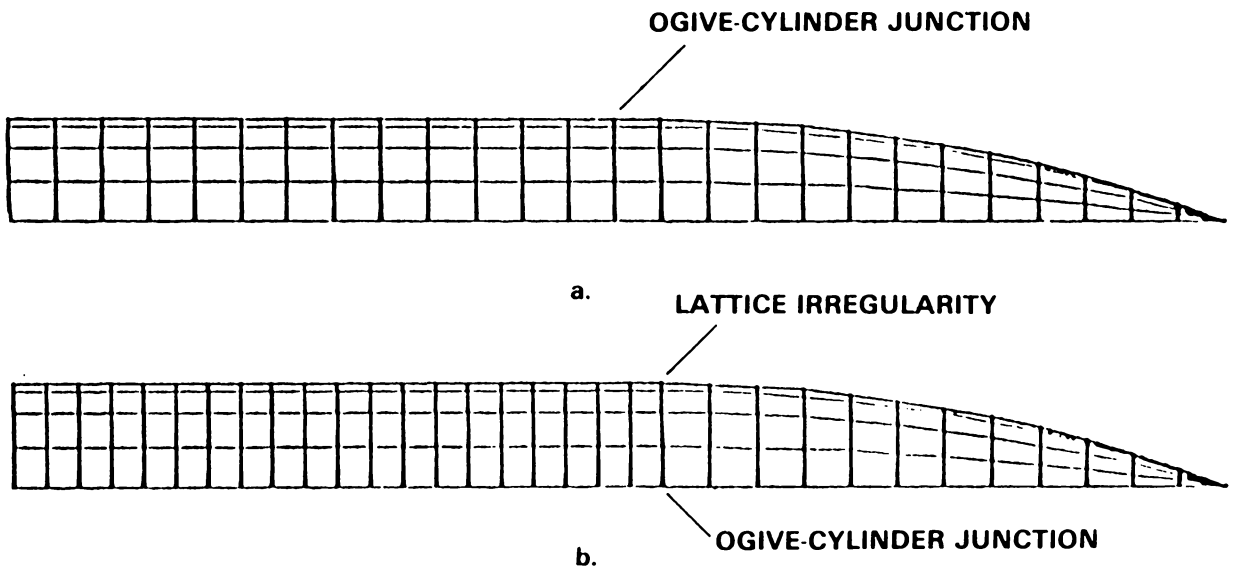

Figure 4-2 Planview of uniform and nonuniform lattices.

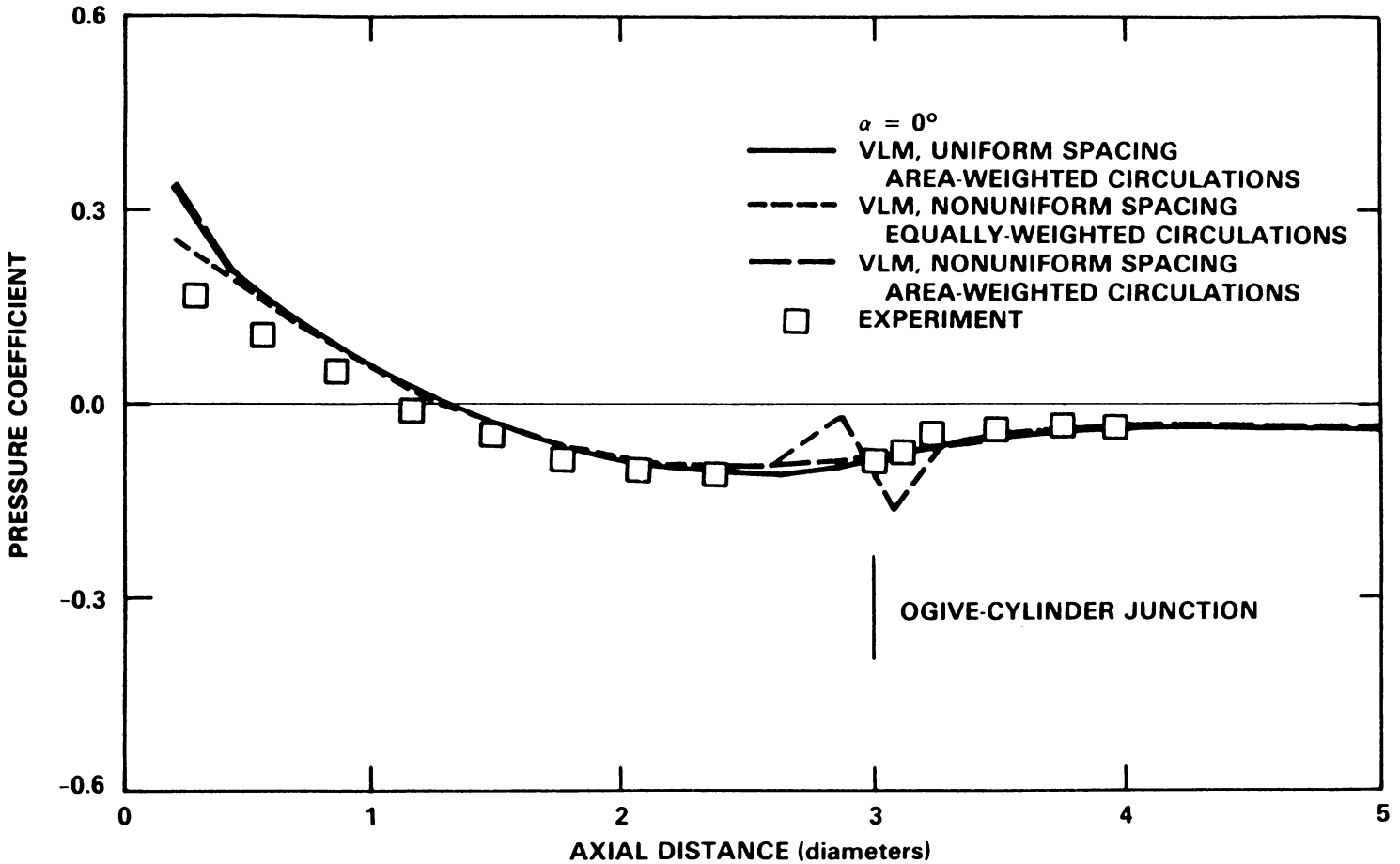

Figure 4-3 Effect of area-weighting branch circulations with an irregularity in the bound-vortex lattice with experiments of Faulkner, Hess, and Giesing (1964).

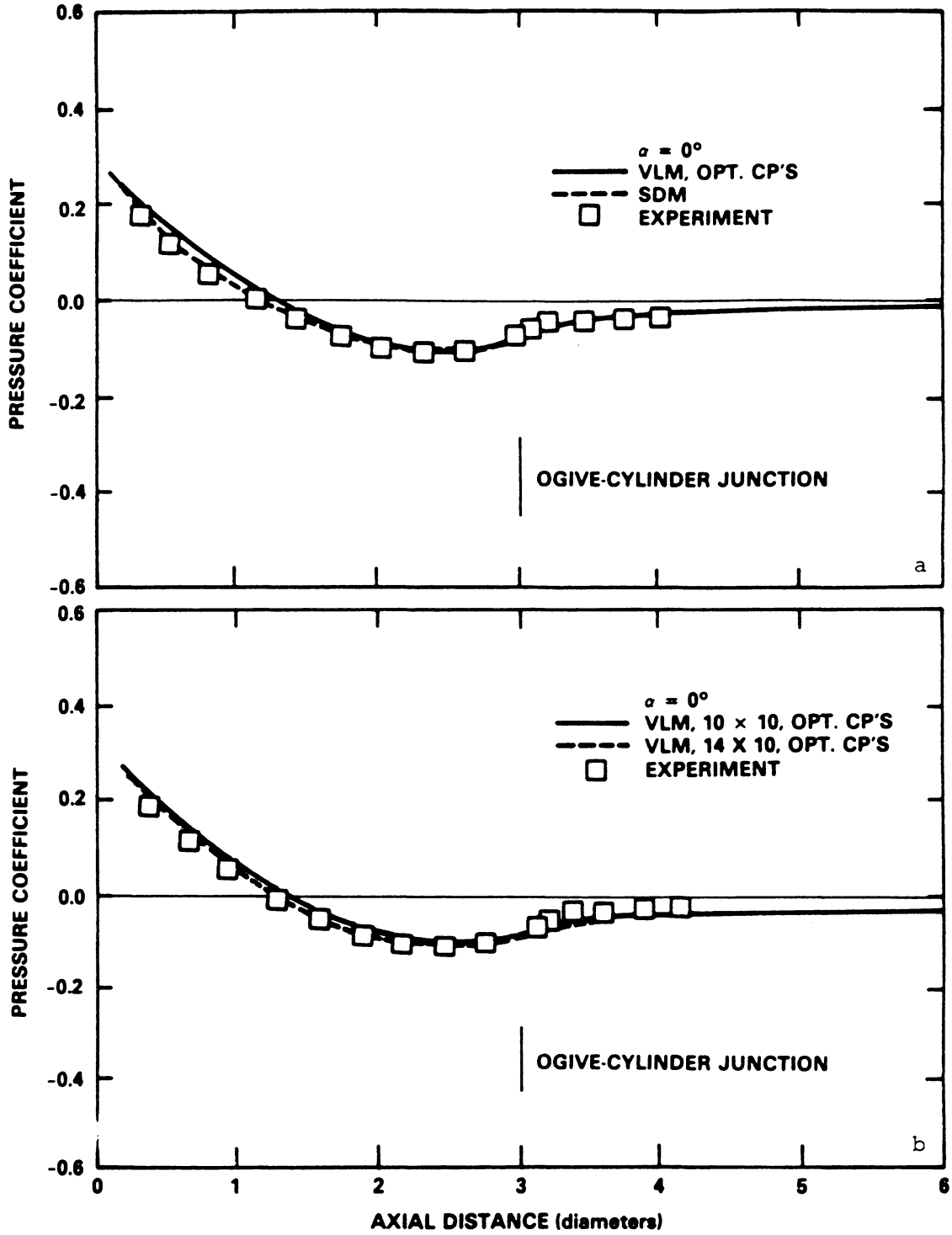

Figure 4-4 Pressure coefficient vs. axial distance calculated with the VLM and the SDM (a) and the effect of axial panel density on the VLM (b) for $\alpha = 0^{\circ}$ with experimental results of Faulkner, Hess, and Giesing (1964).

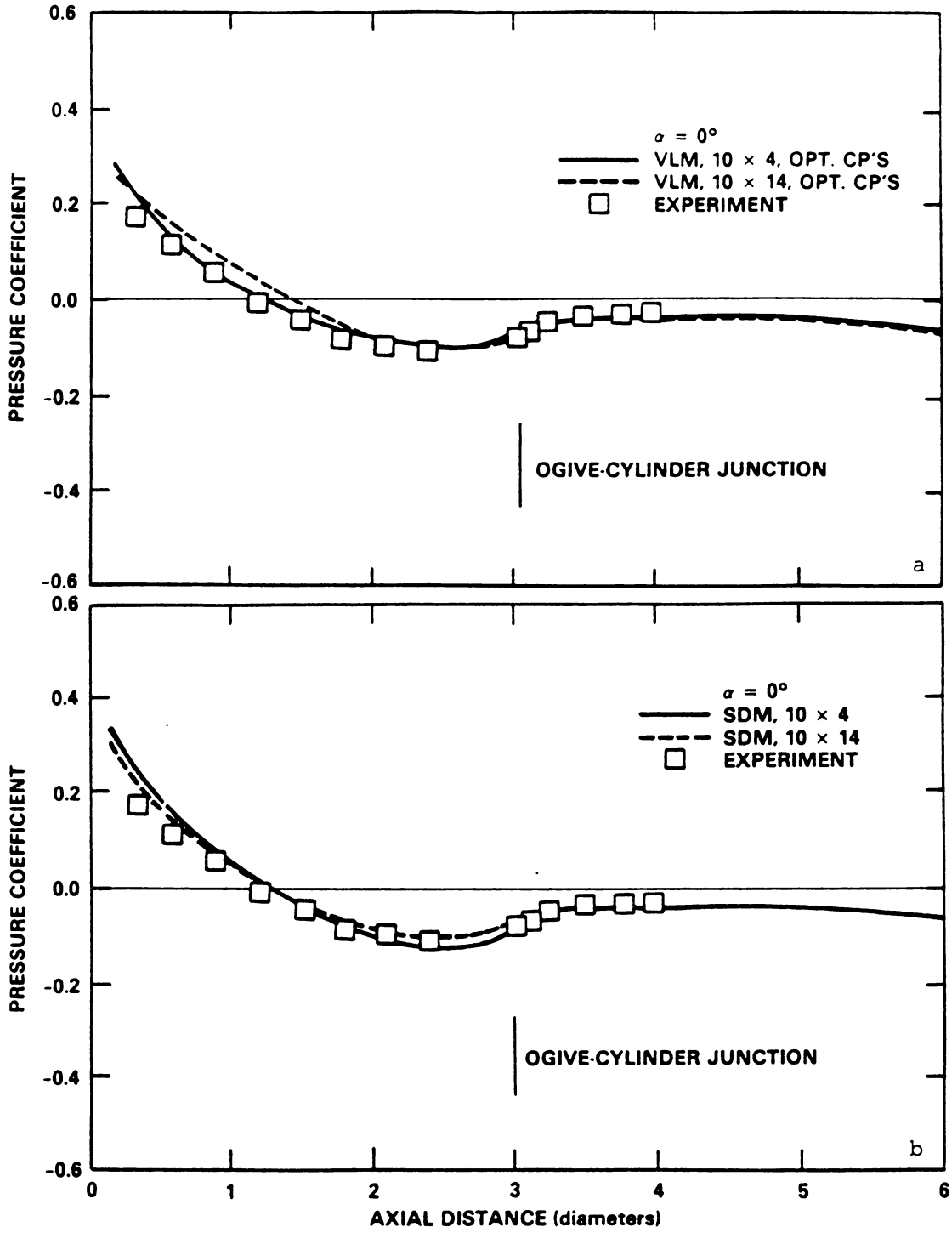

Figure 4-5 Effect of circumferential density of elements in the VLM (a) and the SDM (b) for $\alpha = 0^{\circ}$ with experimental results of Faulkner, Hess, and Giesing (1964).

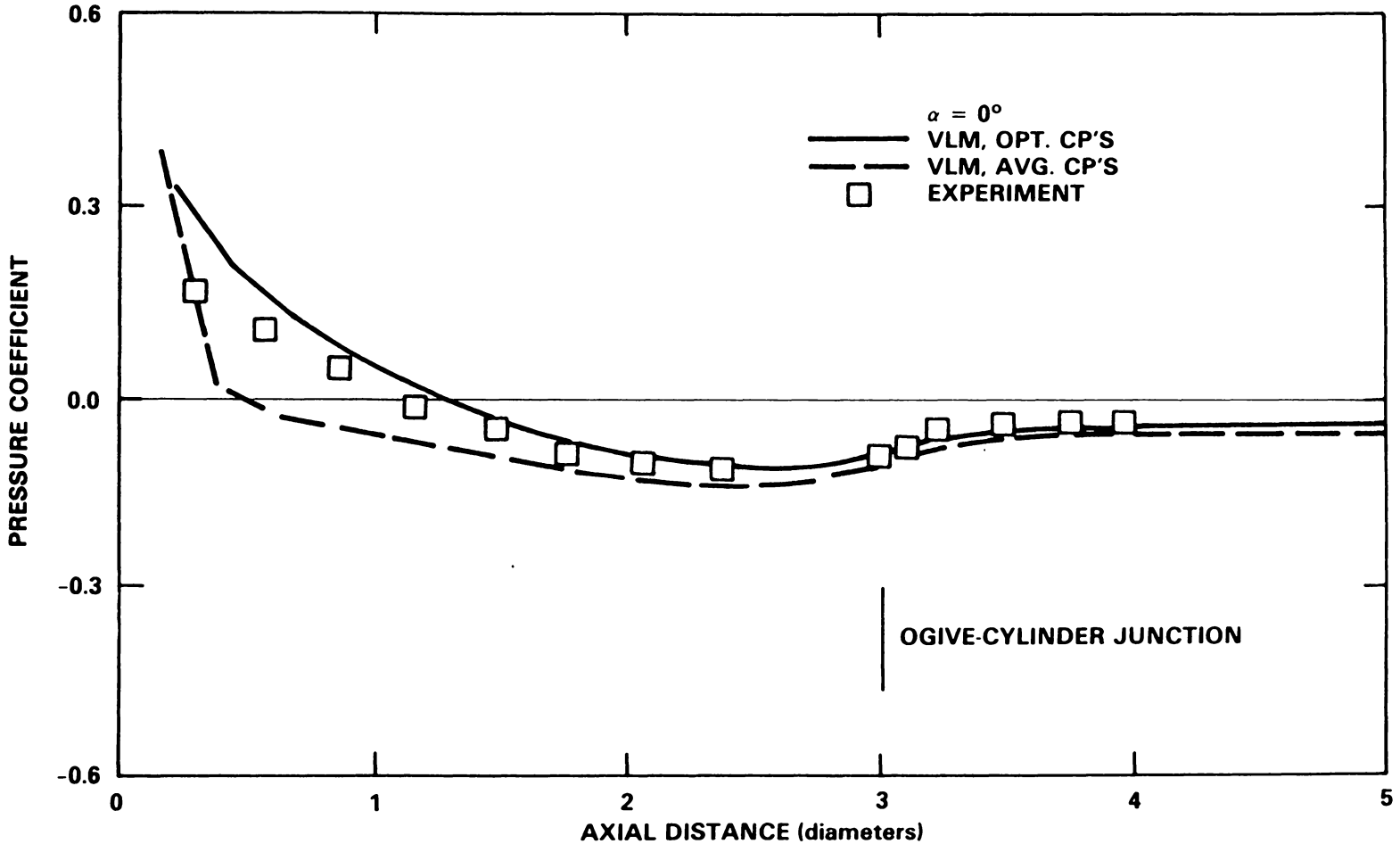

Figure 4-6 Effect of control point location in the VLM for $\alpha = 0^{\circ}$ with experiments of Faulkner, Hess, and Giesing (1964).

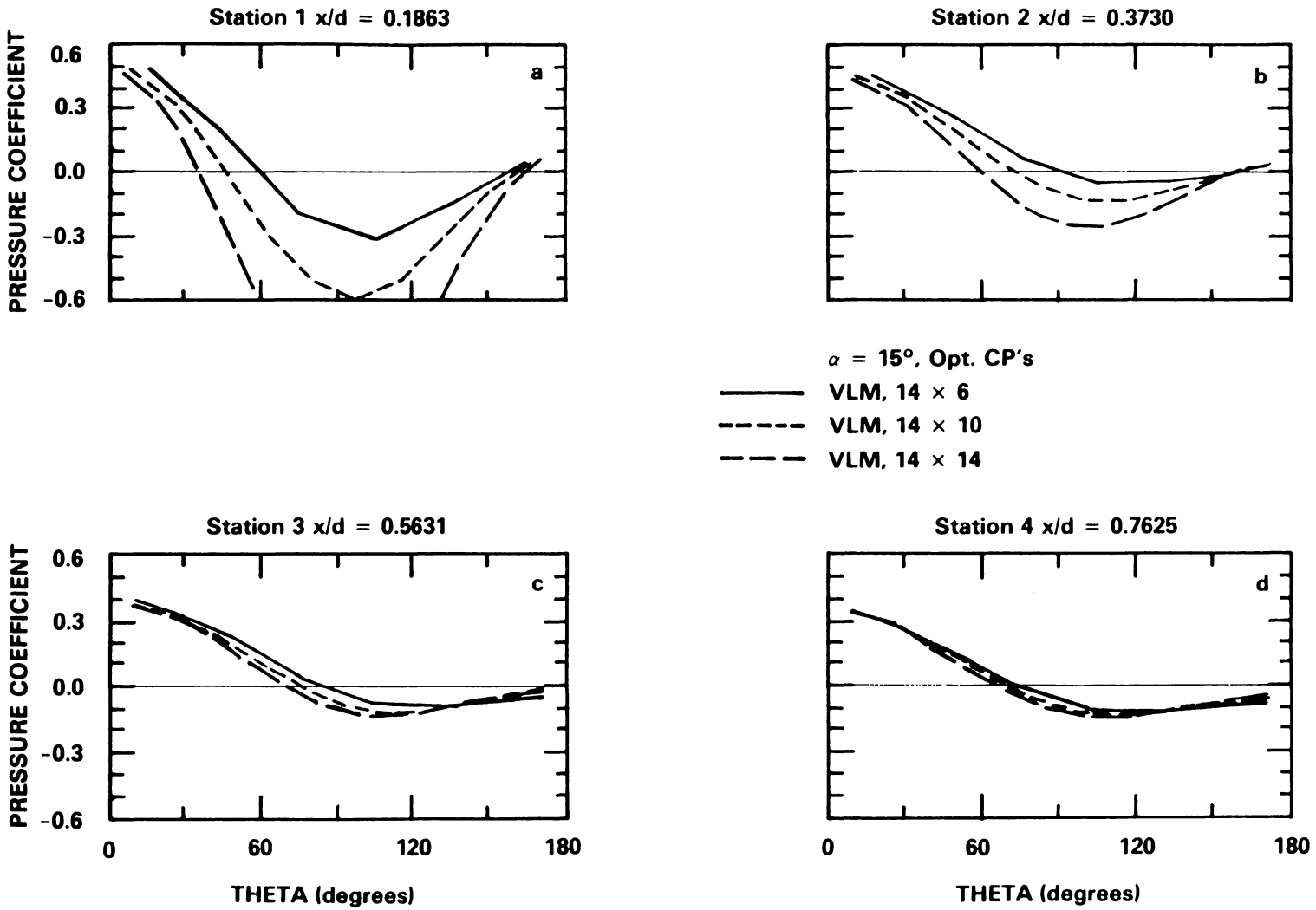

Figure 4-7 Effect of circumferential density of elements in the VLM using optimal control points for $\alpha = 15^{\circ}$.

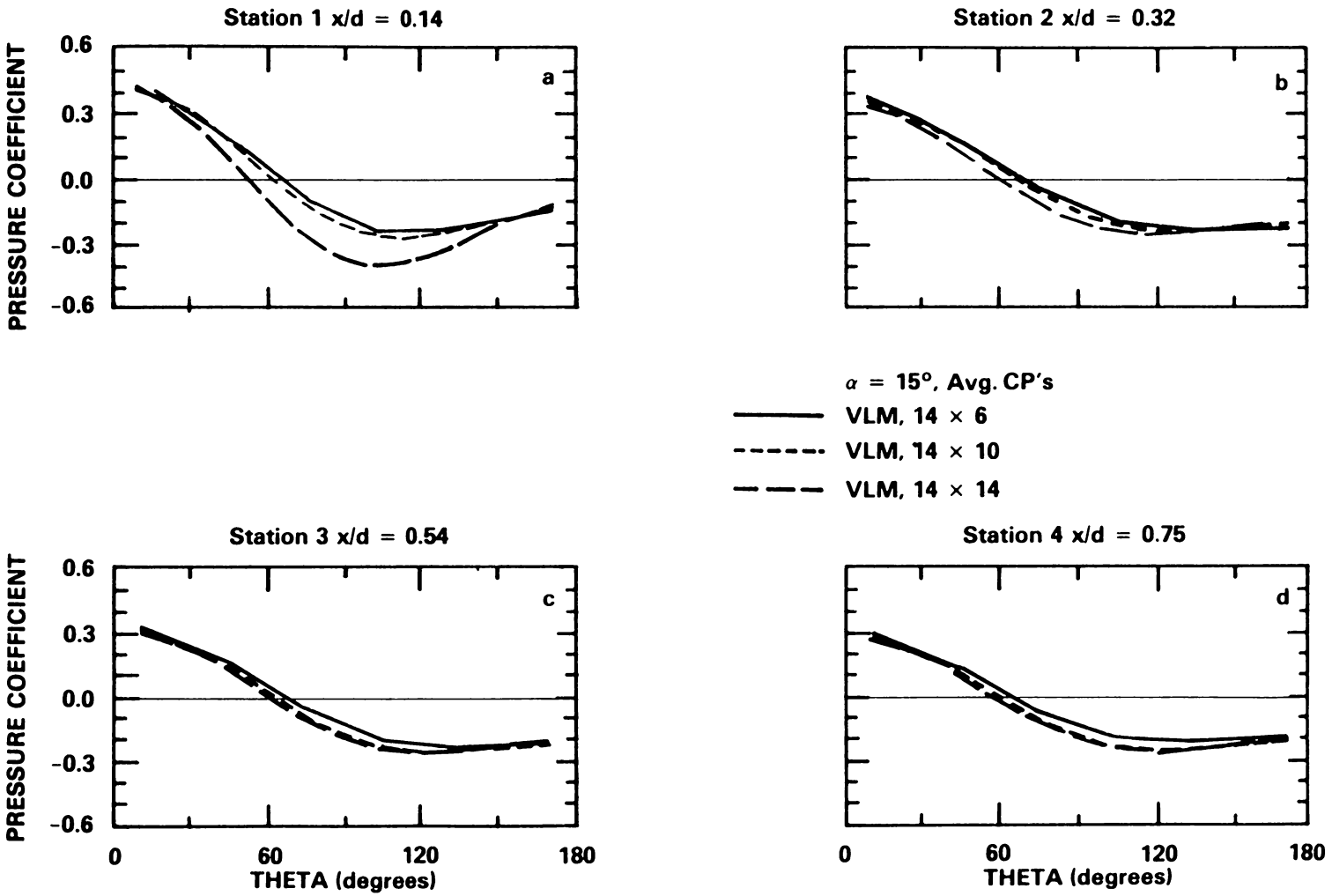

Figure 4-8 Effect of circumferential density of elements in the VLM using average control points for $\alpha = 15^{\circ}$.

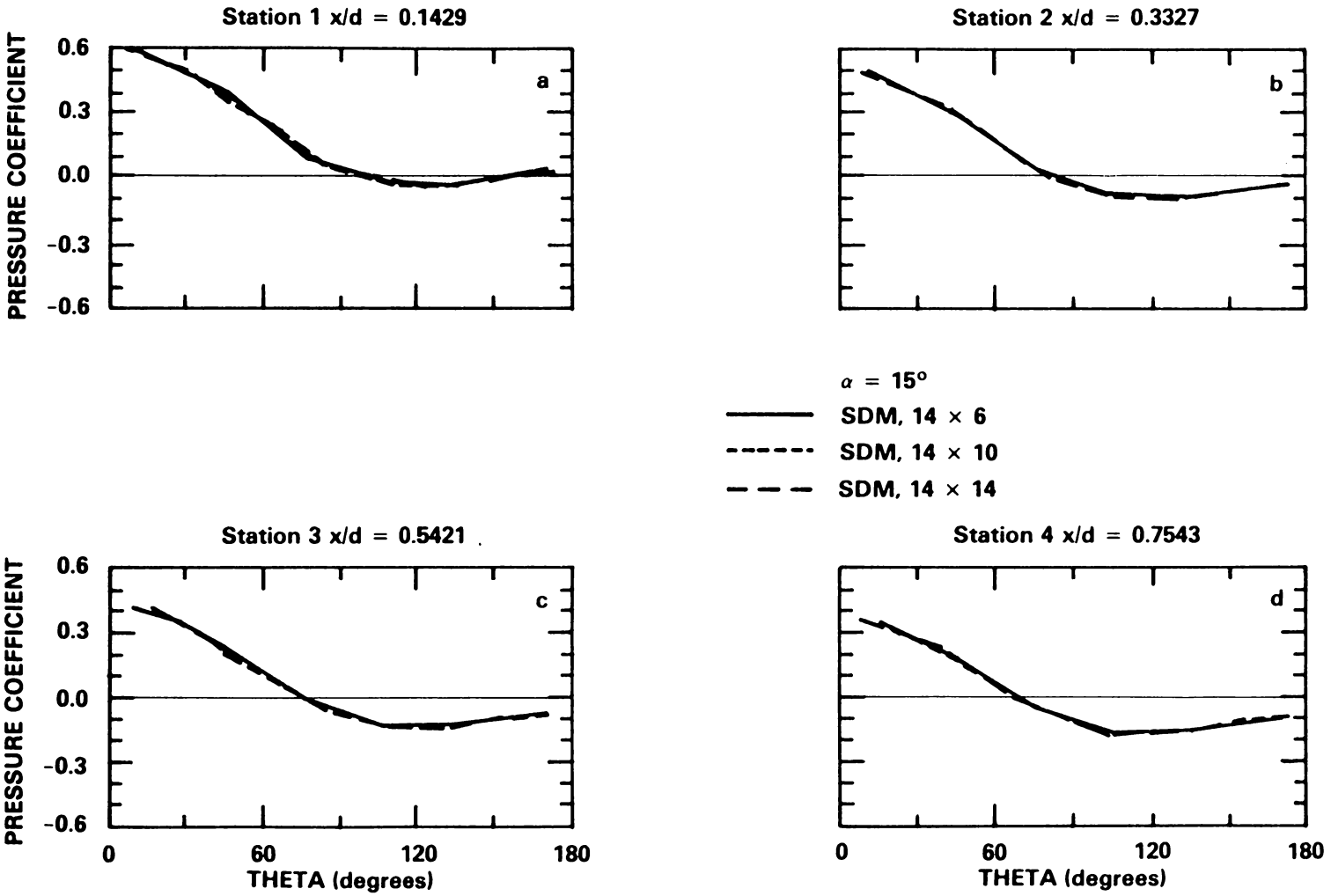

Figure 4-9 Effect of circumferential density of elements in the SDM for $\alpha = 15^{\circ}$.

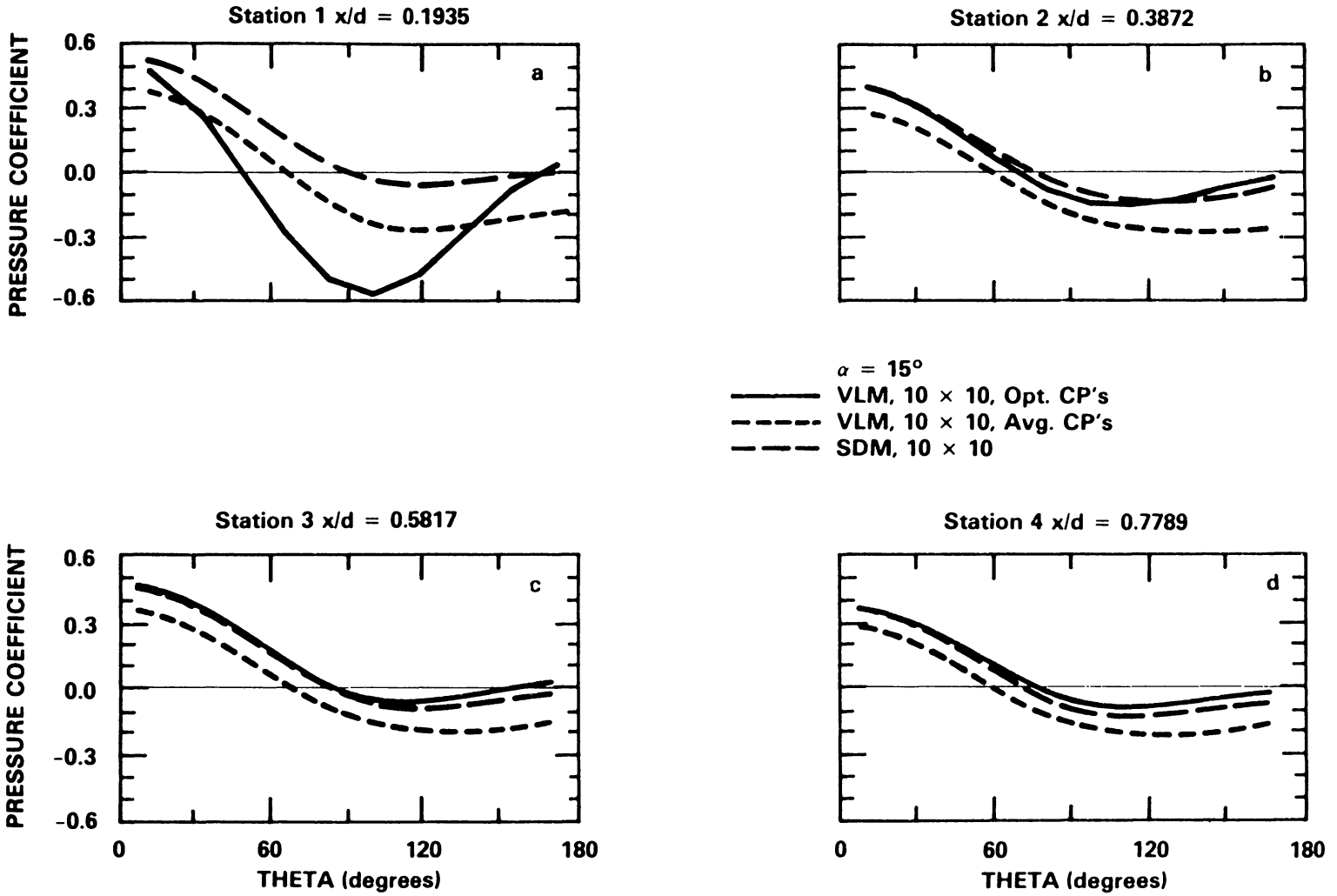

Figure 4-10 Effect of circumferential density of elements in the VLM and the SDM for $\alpha = 15^{\circ}$.

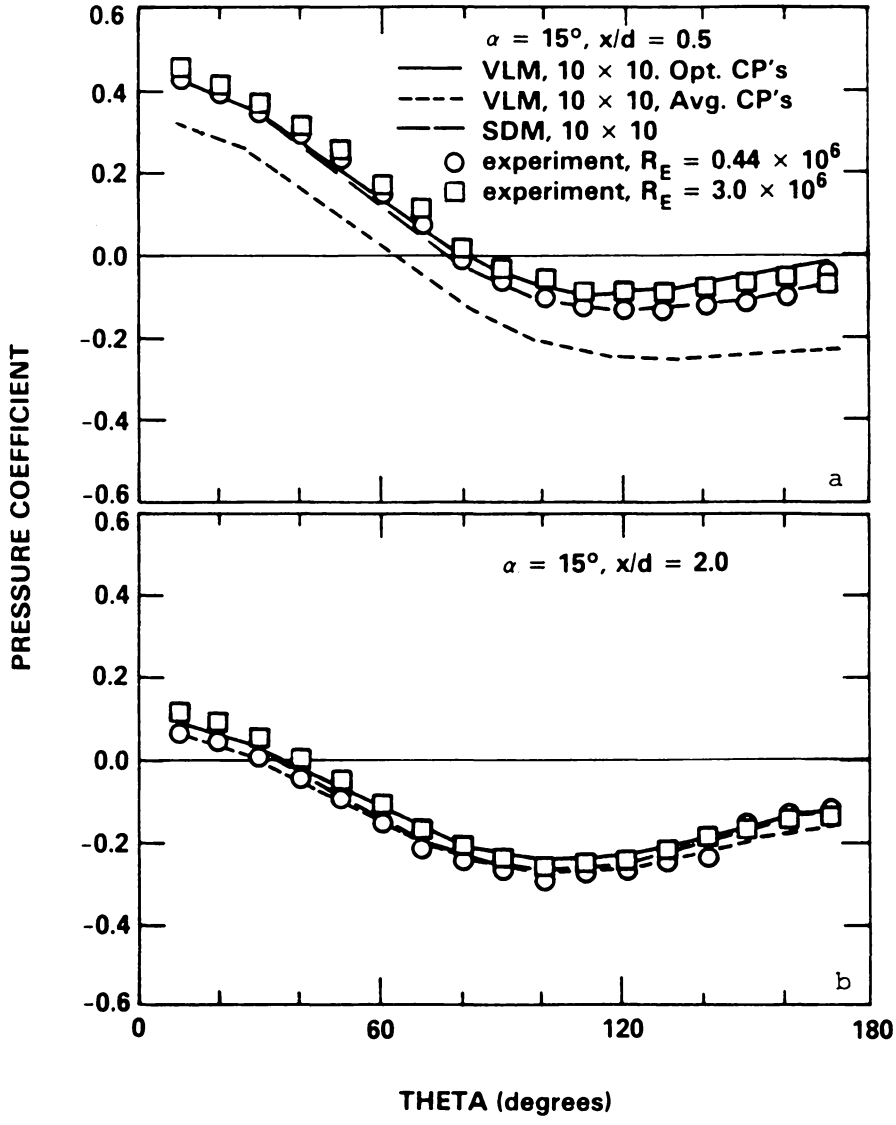

Figure 4-11 Calculated attached pressure coefficients with the experimental results of Tinling and Allen (1962) for x/d = .5(a) and 2.(b) for $\alpha = 15^{\circ}$.

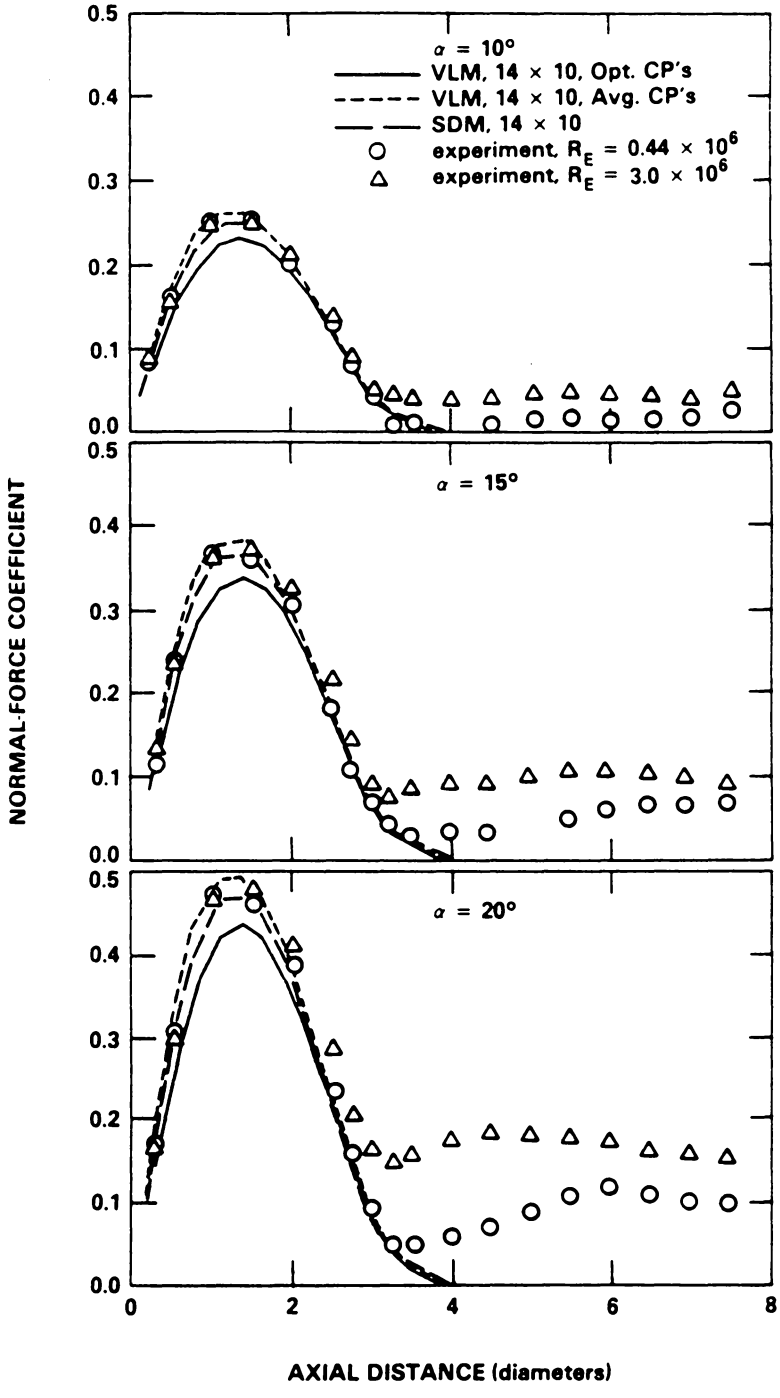

Figure 4-12 Calculated attached normal-force coefficient with the experimental results of Tinling and Allen (1962) for $\alpha = 10^{\circ}$, 15°, and 20°.

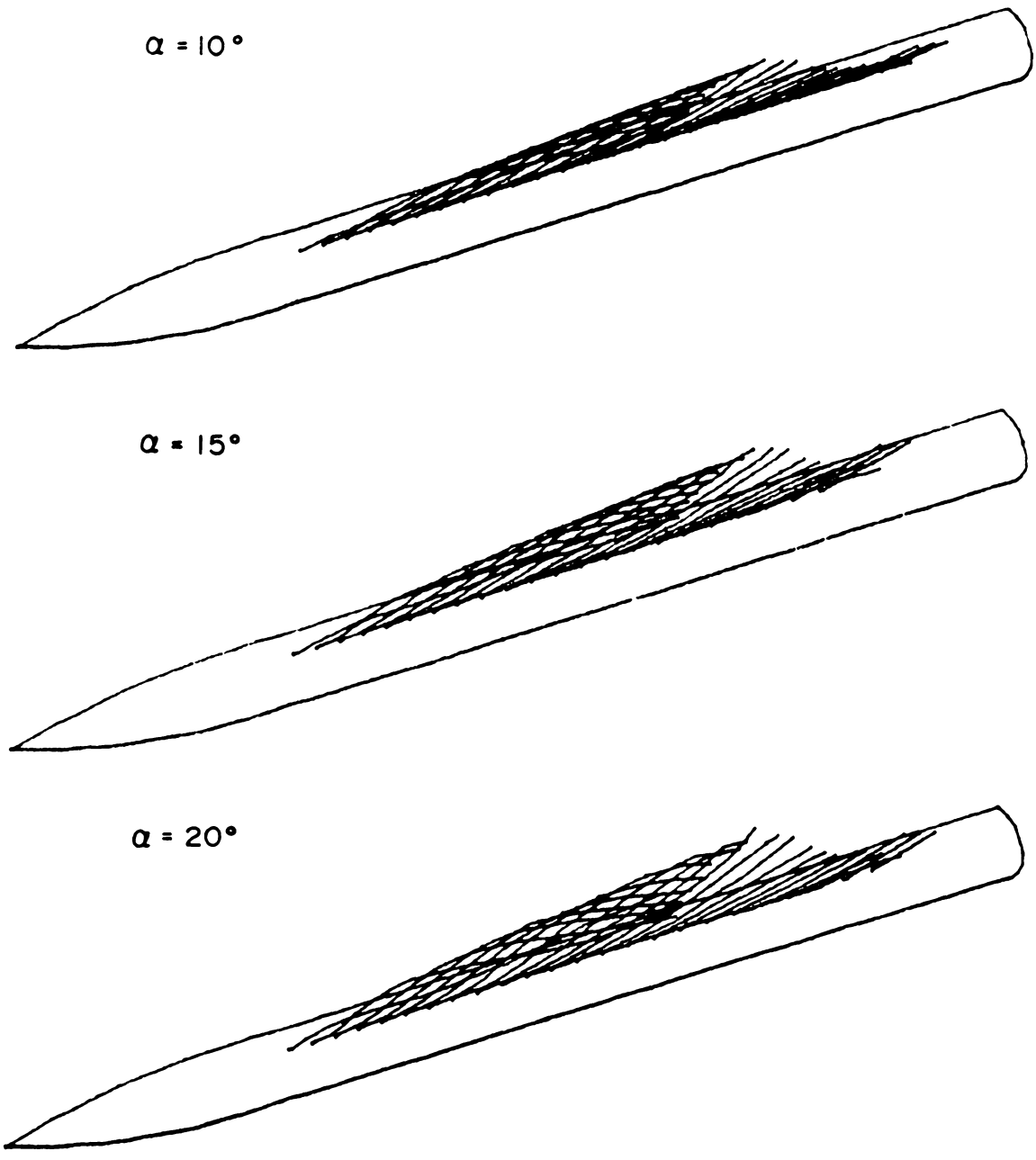

Figure 4-13 Perspective view of calculated vortex wakes for $\alpha = 10^{\circ}$, 15°, and 20°.

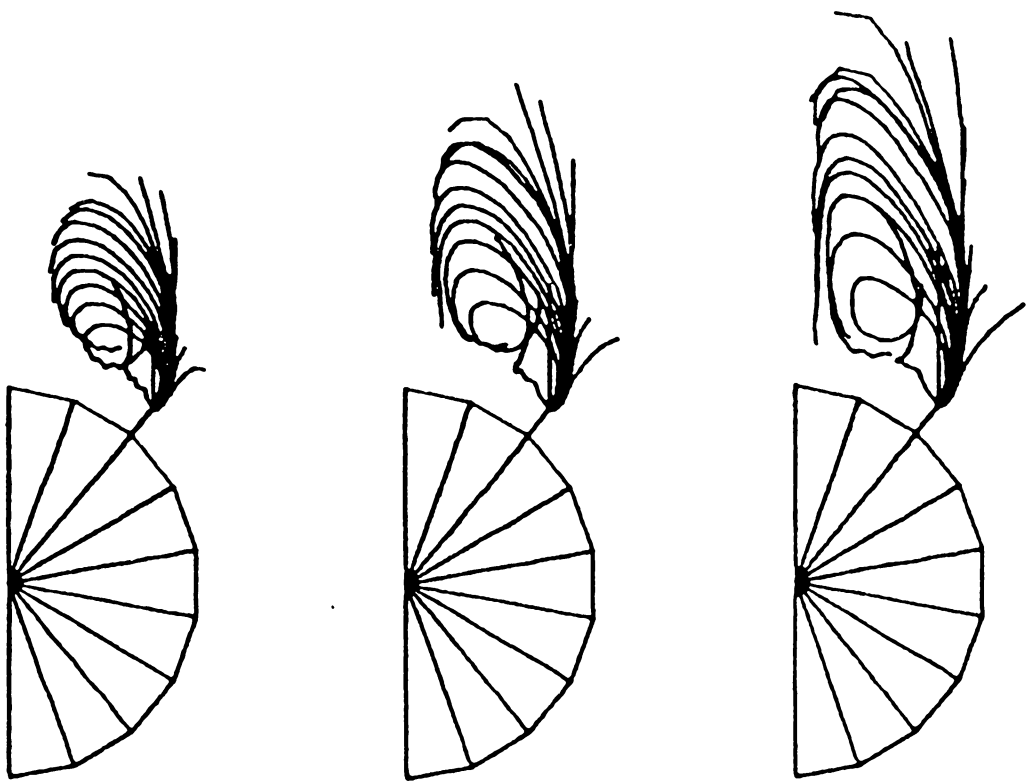

Figure 4-14 Front view of calculated vortex wakes for $\alpha = 10^{\circ}$, 15°, and 20°.

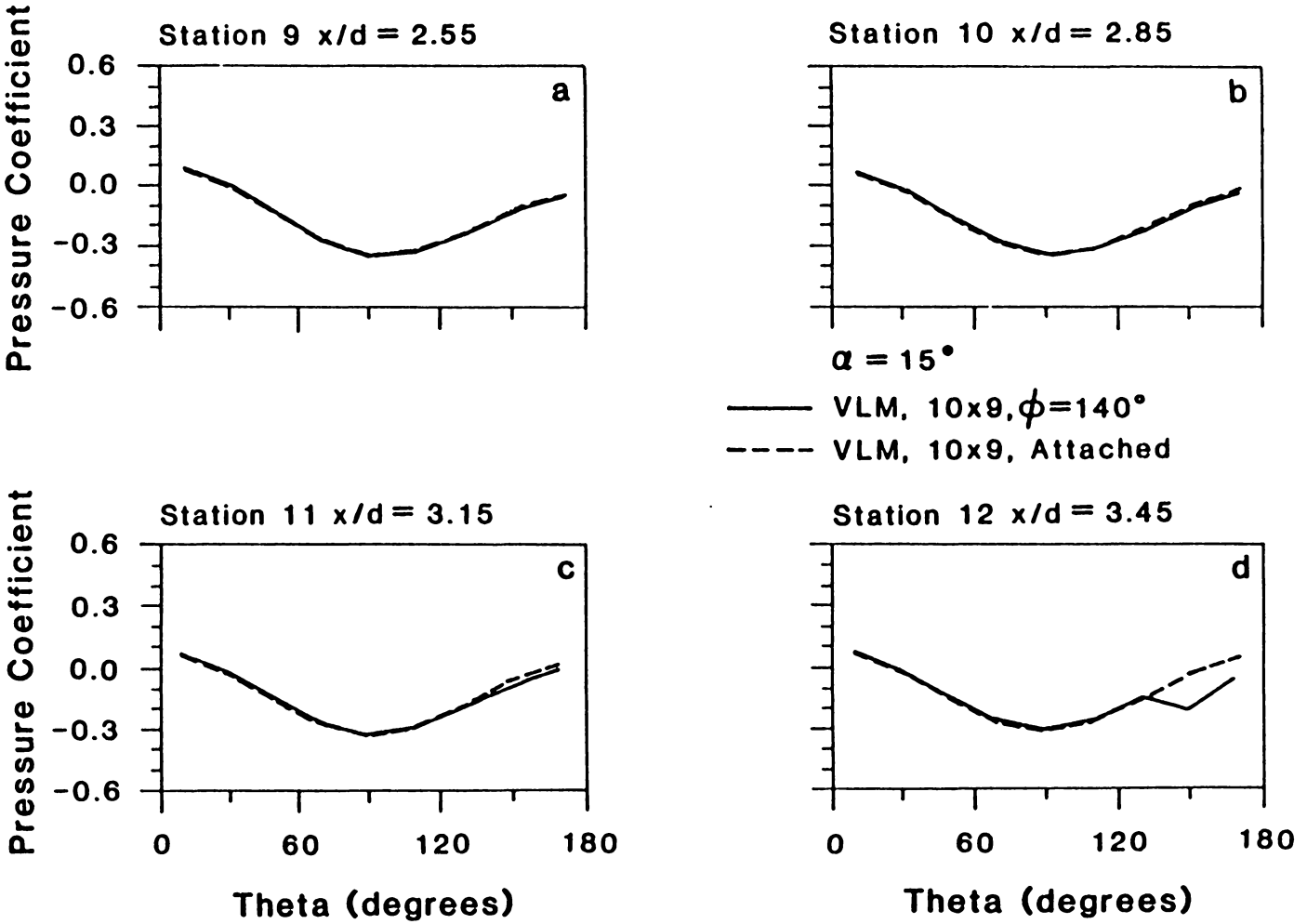

Figure 4-15 Calculated attached and separated flow pressure coefficient for calculation stations 9 through 12 for $\alpha = 15^{\circ}$.

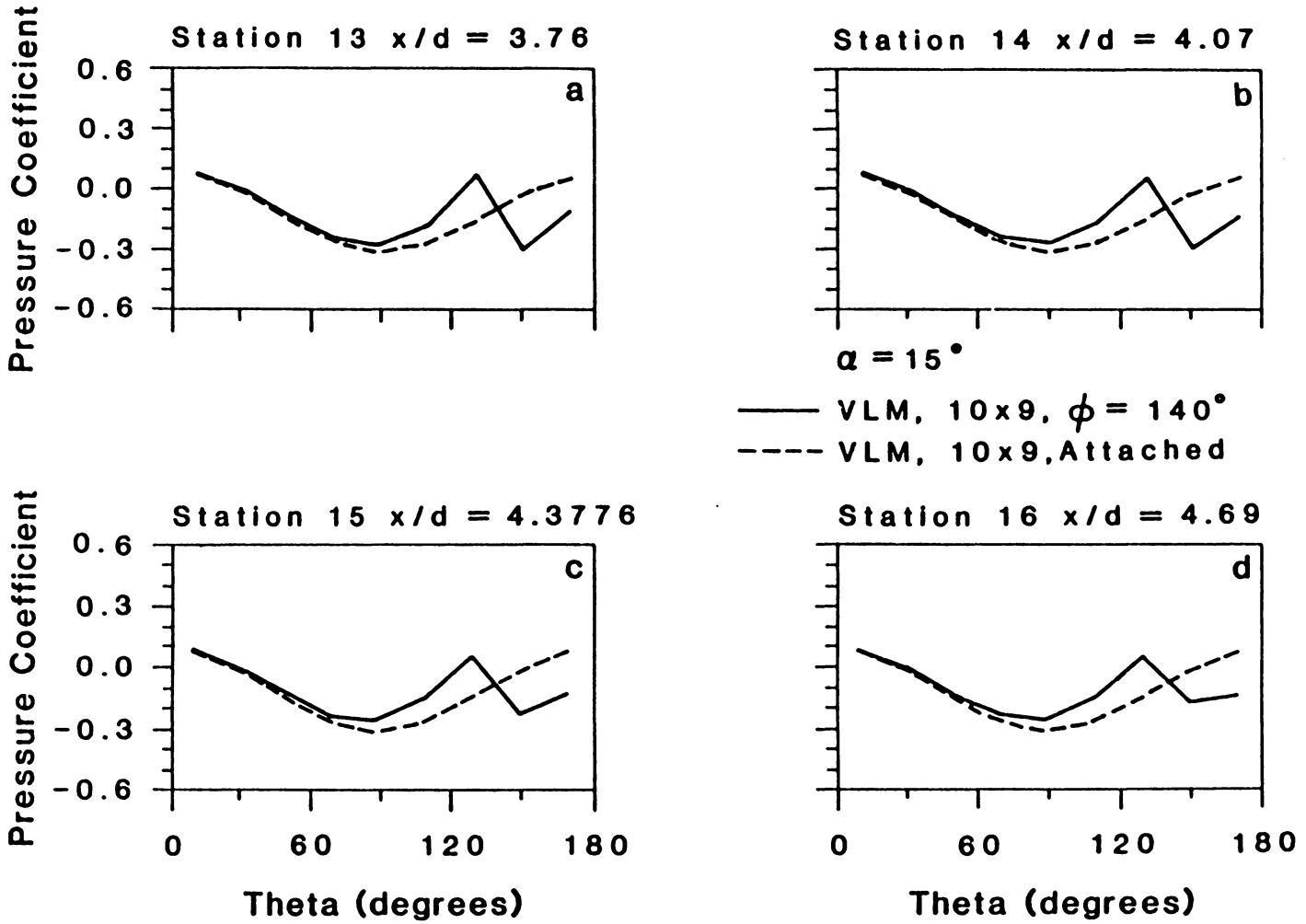

Figure 4-16 Calculated attached and separated flow pressure coefficient for calculation stations 13 through 16, for $\alpha = 15^{\circ}$.

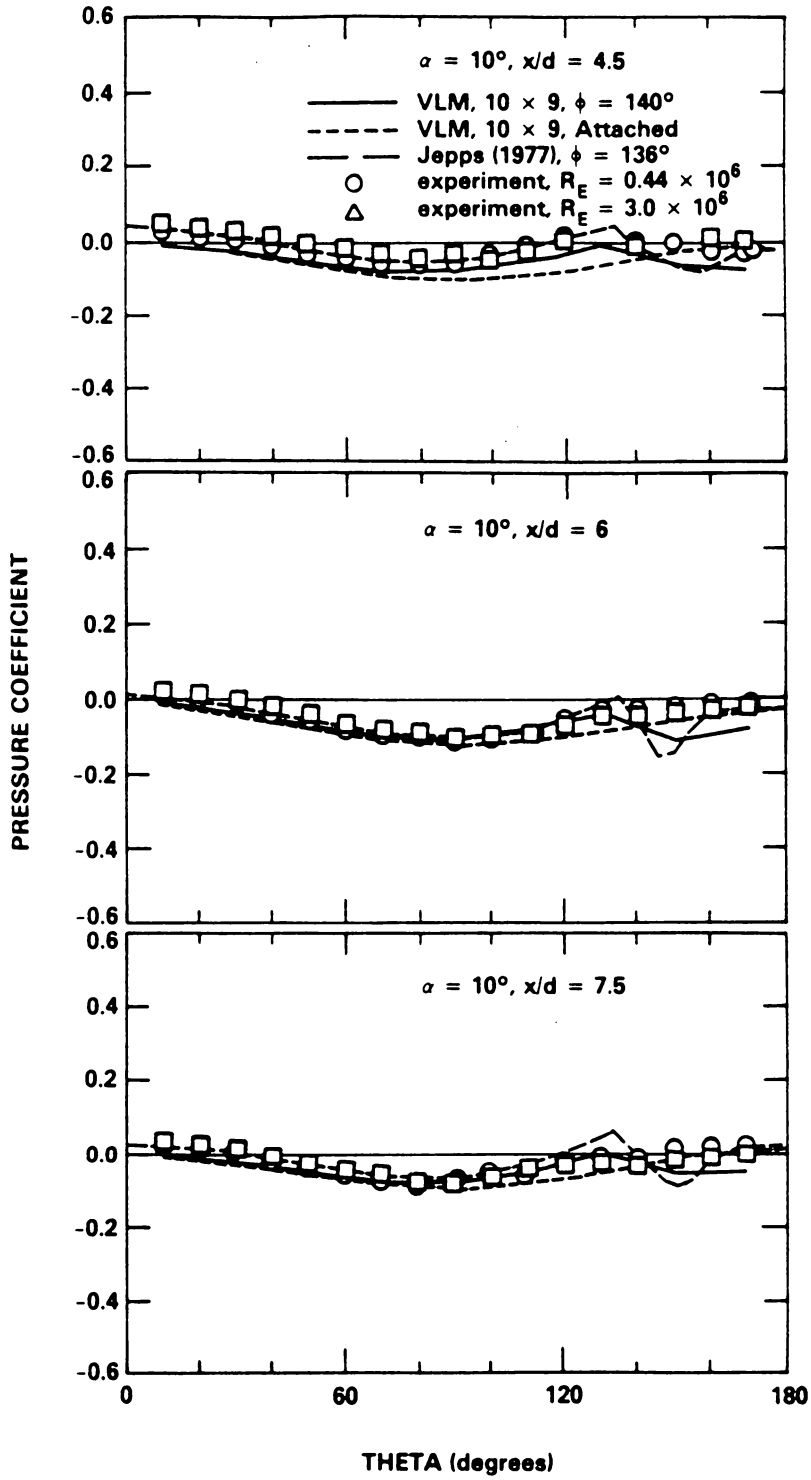

Figure 4-17 Calculated attached and separated pressure coefficient with calculations of Jepps (1977) and experimental results of Tinling and Allen (1962) for x/d = 4.5, 6., and 7.5 for $\alpha = 10^{\circ}$, $\phi = 140^{\circ}$.

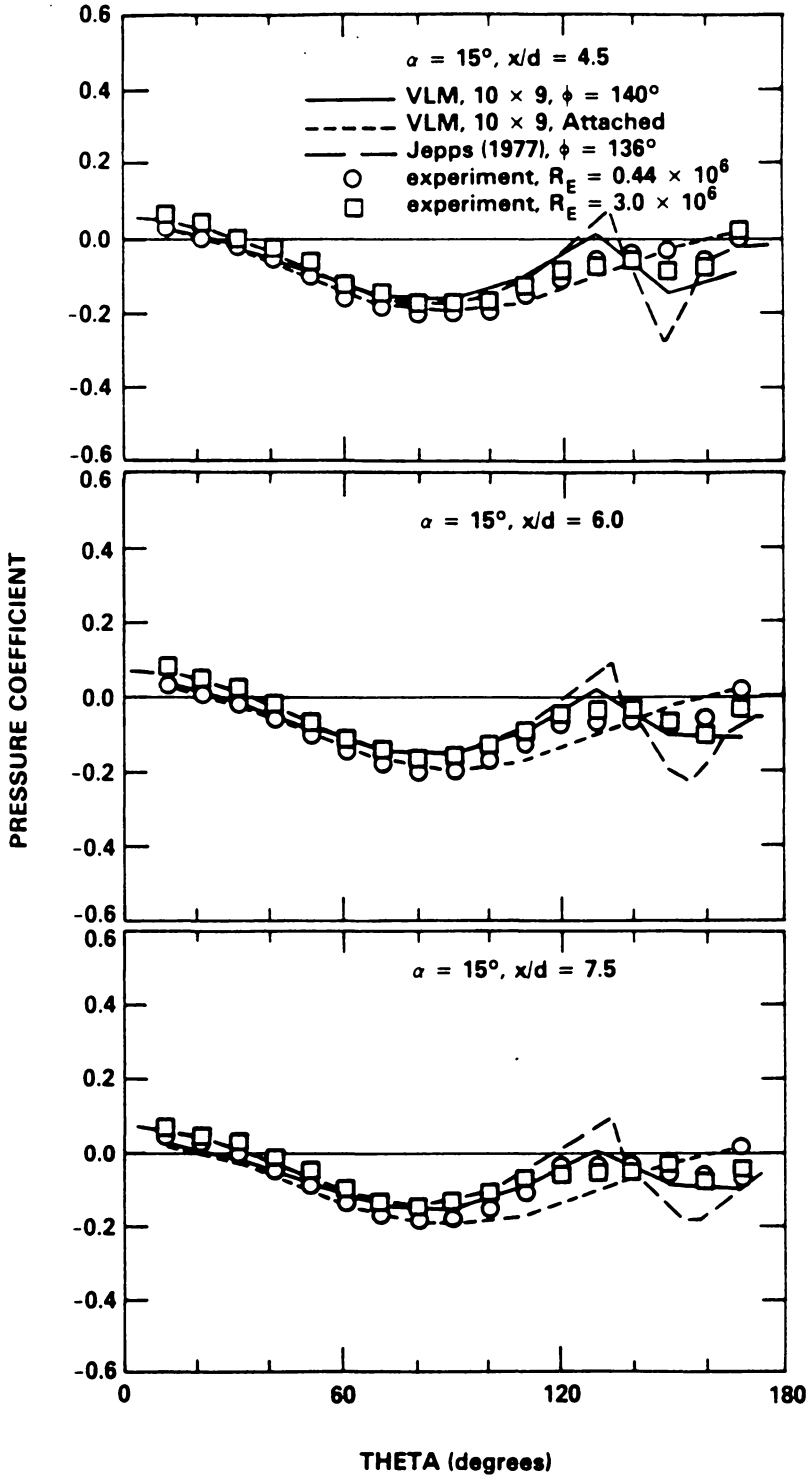

Figure 4-18 Calculated attached and separated pressure coefficient with calculations of Jepps (1977) and experimental results of Tinling and Allen (1962) for x/d = 4.5, 6., and 7.5 for $\alpha = 15^{\circ}$, $\phi = 140^{\circ}$.

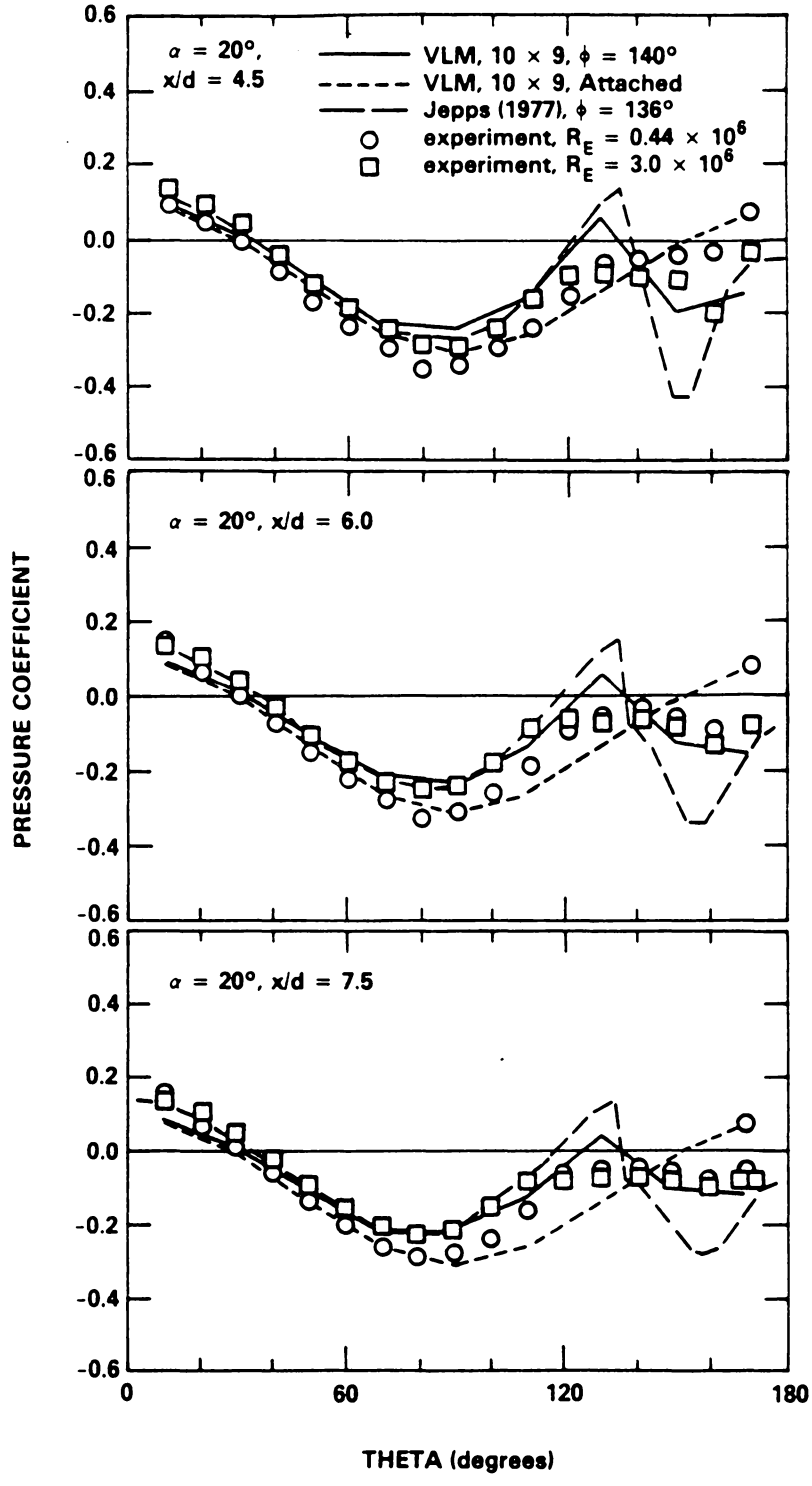

Figure 4-19 Calculated attached and separated pressure coefficient with calculations of Jepps (1977) and experimental results of Tinling and Allen (1962) for x/d = 4.5, 6., and 7.5 for $\alpha = 20^{\circ}$, $\phi = 140^{\circ}$.

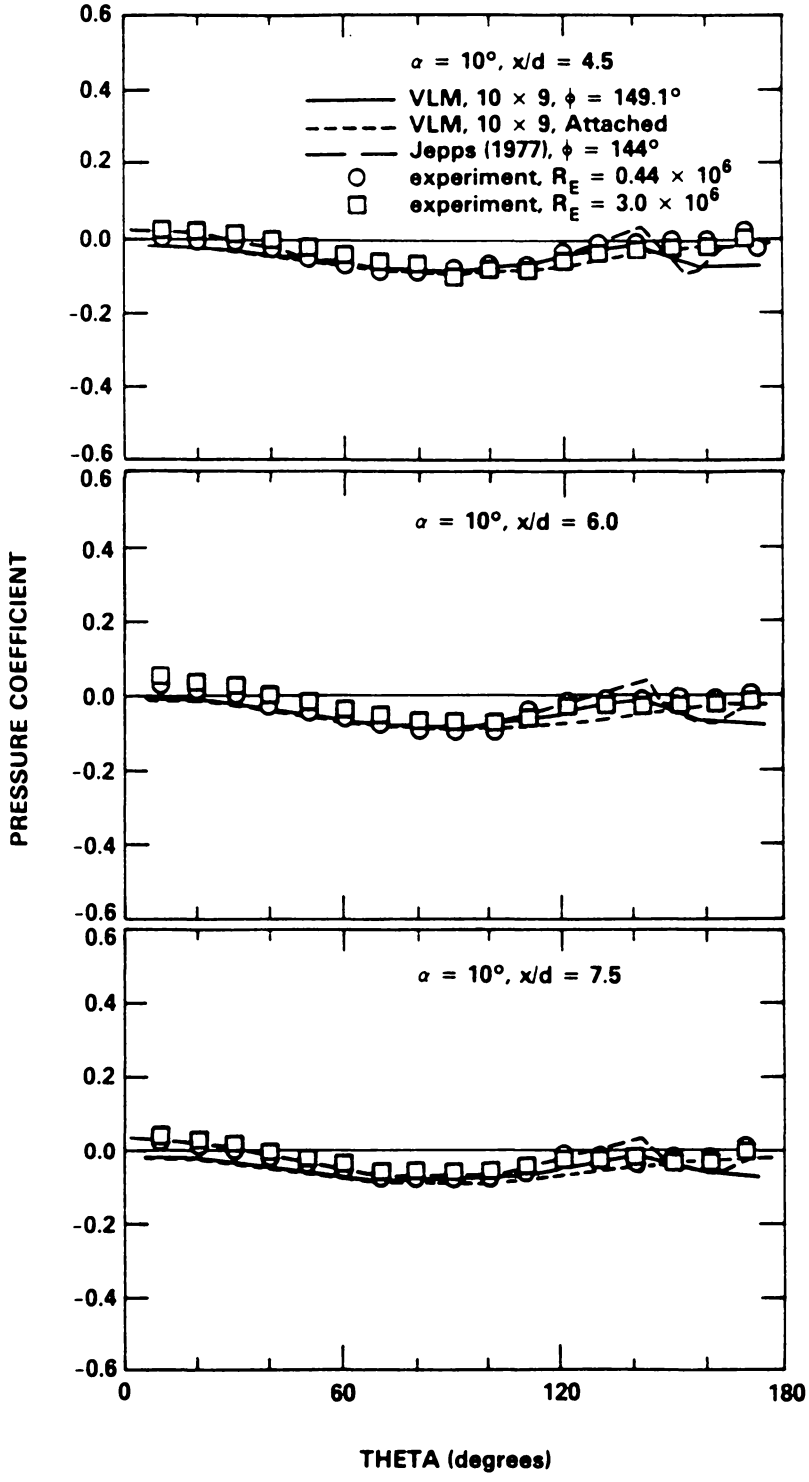

Figure 4-20 Calculated attached and separated pressure coefficient with calculations of Jepps (1977) and experimental results of Tinling and Allen (1962) for x/d = 4.5, 6., and 7.5 for $\alpha = 10^{\circ}$, $\phi = 149.1^{\circ}$.

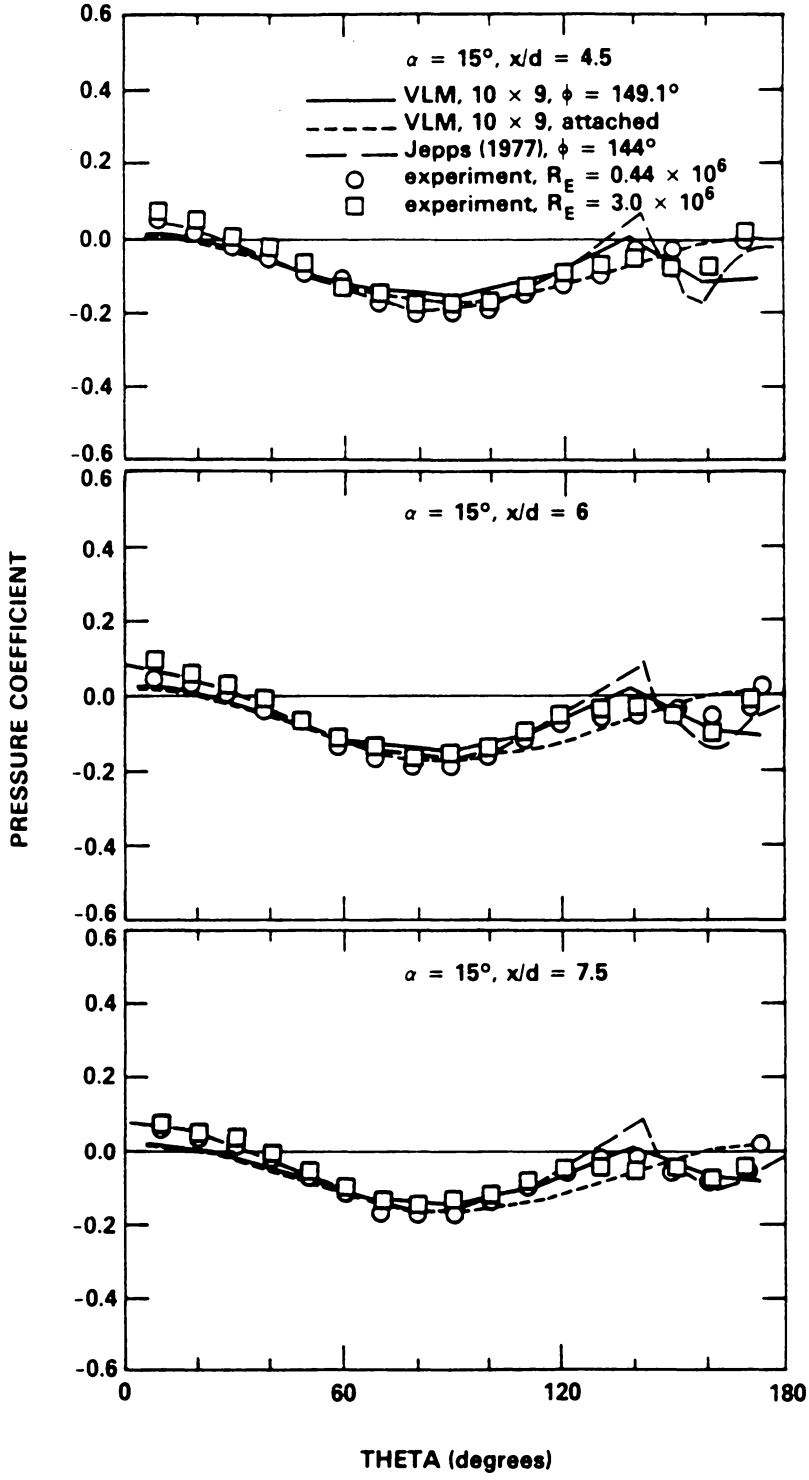

Figure 4-21 Calculated attached and separated pressure coefficient with calculations of Jepps (1977) and experimental results of Tinling and Allen (1962) for x/d = 4.5, 6., and 7.5 for $\alpha = 15^{\circ}$, $\phi = 149.1^{\circ}$.

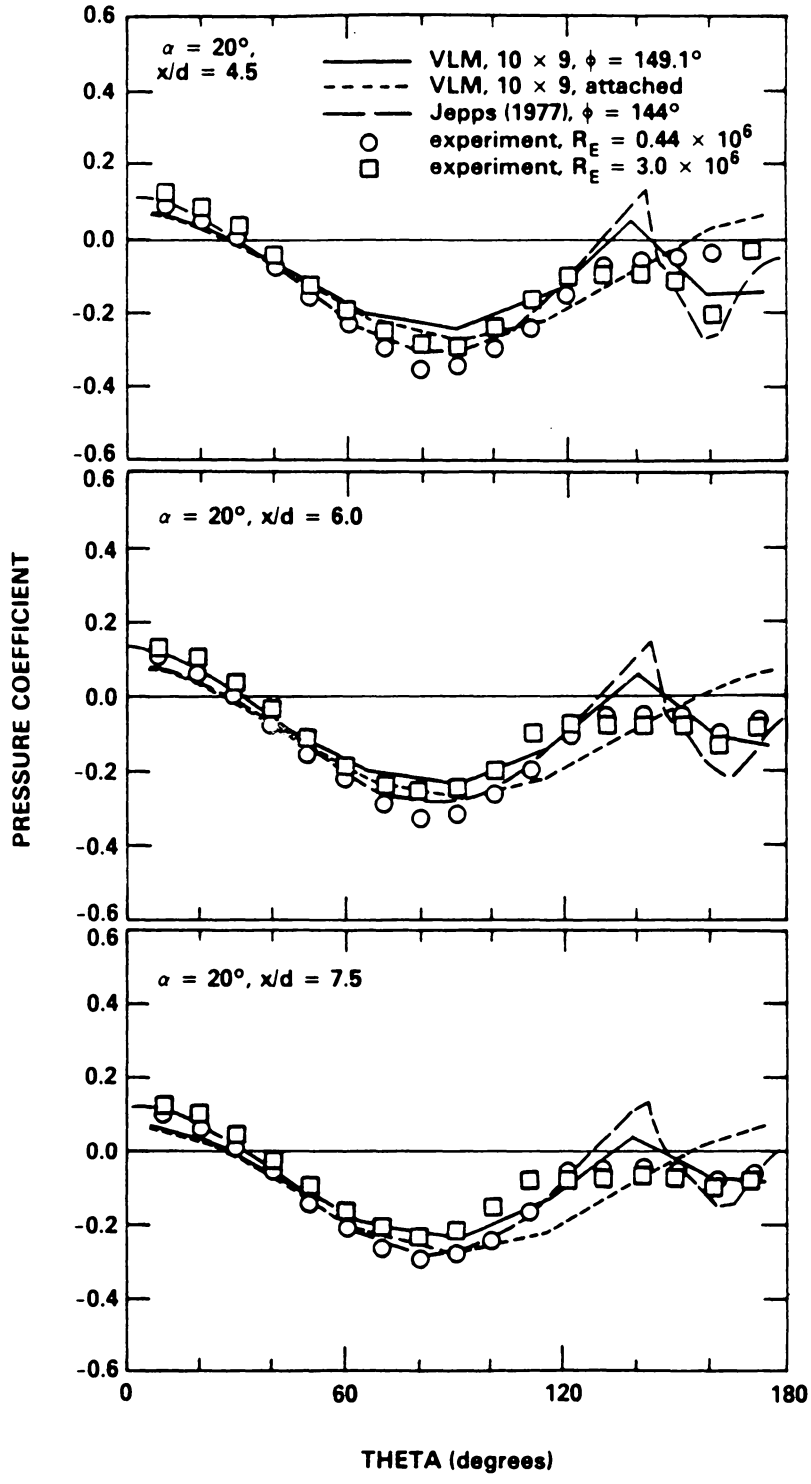

Figure 4-22 Calculated attached and separated pressure coefficient with calculations of Jepps (1977) and experimental results of Tinling and Allen (1962) for x/d = 4.5, 6., and 7.5 for $\alpha = 20^{\circ}$, $\phi = 149.1^{\circ}$.

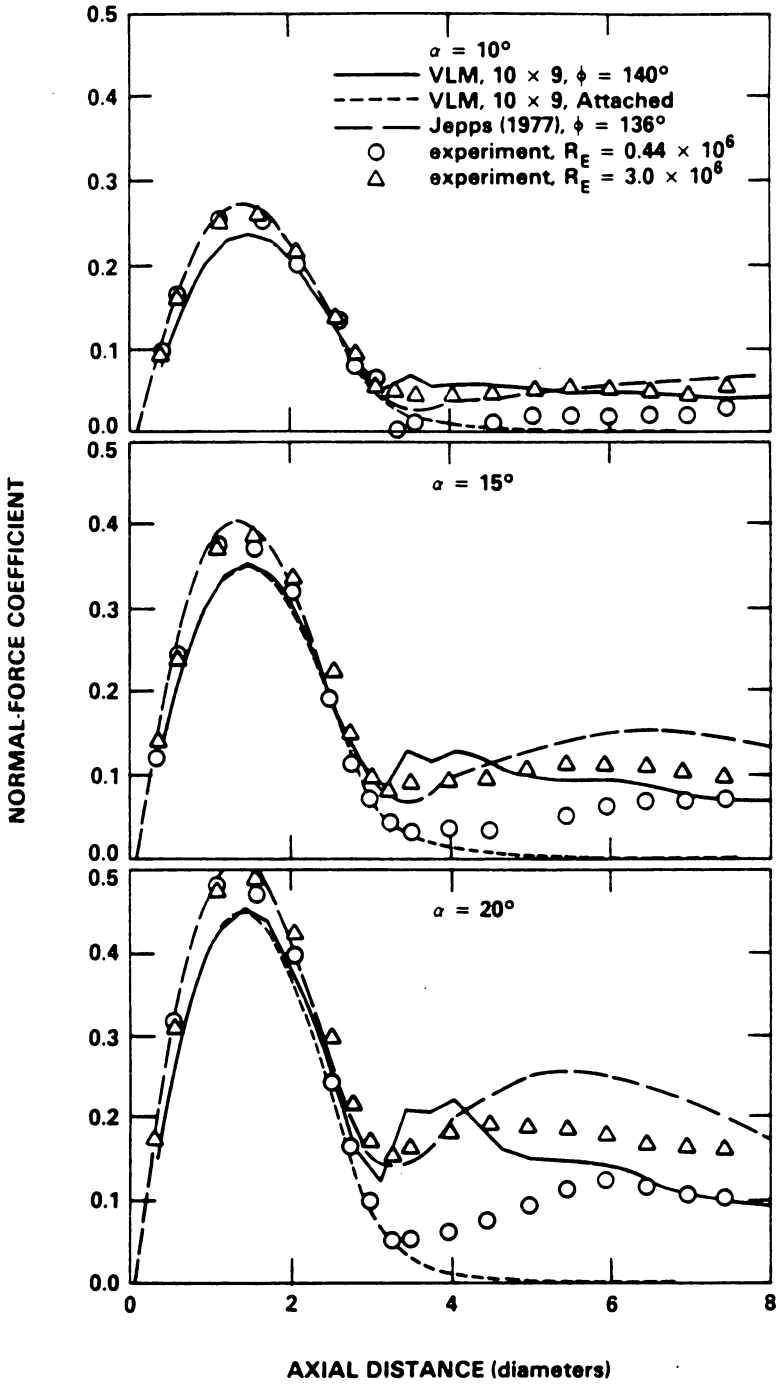

Figure 4-23 Calculated attached and separated normal-force coefficients with calculations of Jepps (1977) and experimental results of Tinling and Allen (1962) for α = 10°, 15°, and 20° for ϕ = 140°.

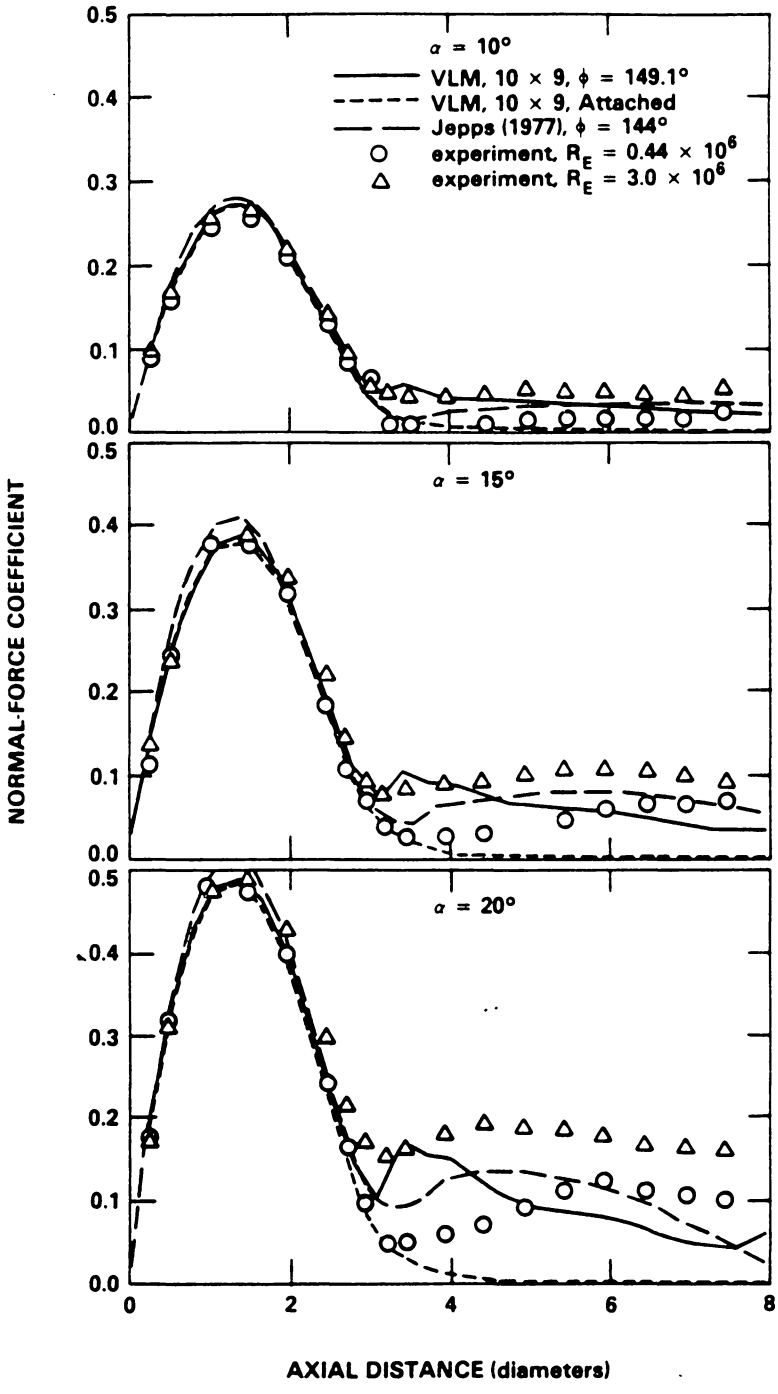

Figure 4-24 Calculated attached and separated normal-force coefficients with calculations of Jepps (1977) and experimental results of Tinling and Allen (1962) for $\alpha = 10^\circ$, 15°, and 20° for $\phi = 149.1^\circ$.

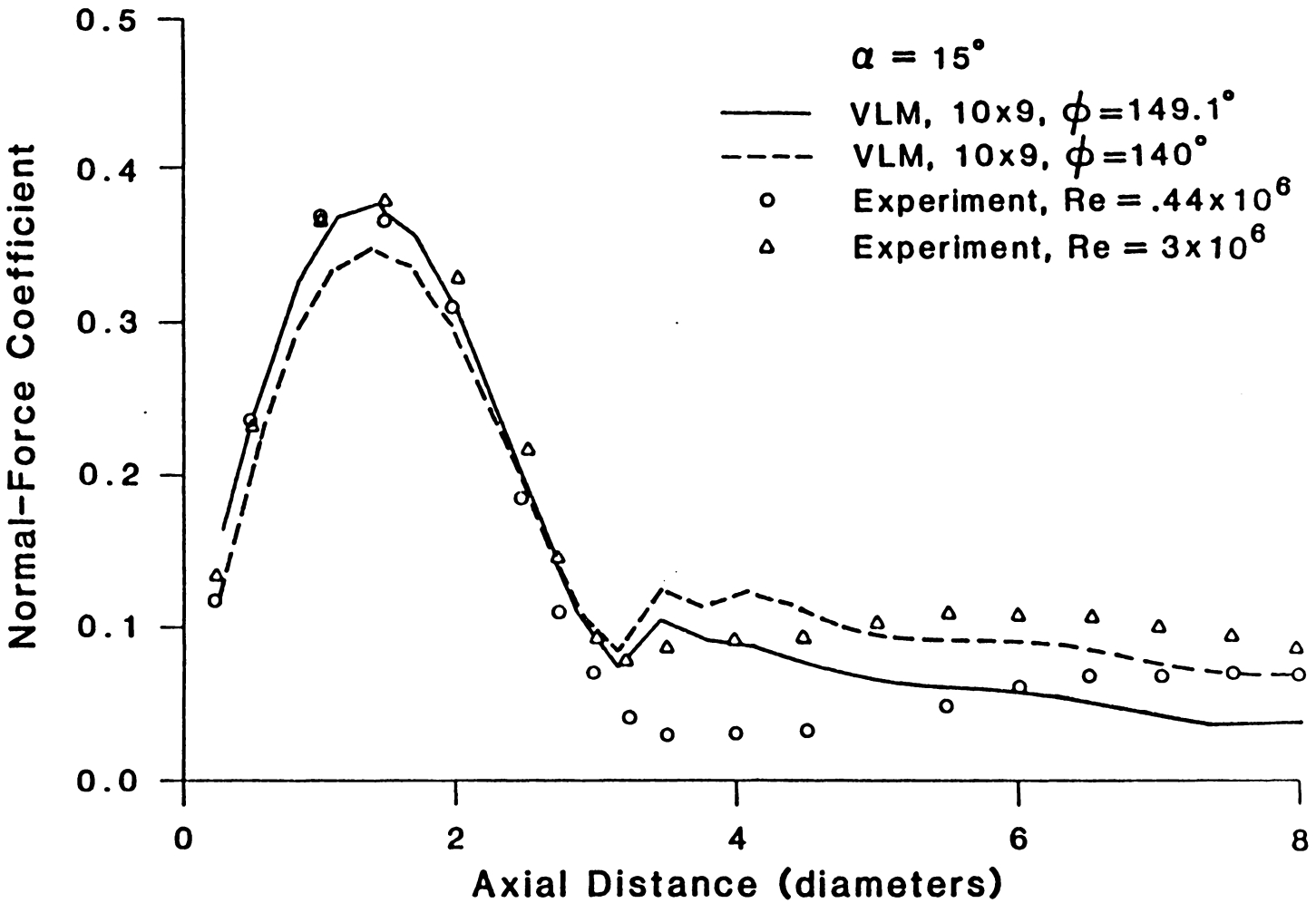

Figure 4-25 Calculated separated normal-force coefficient for $\alpha = 15^{\circ}$, $\phi = 140^{\circ}$ and 149.1° with experimental results of Tinling and Allen (1962).

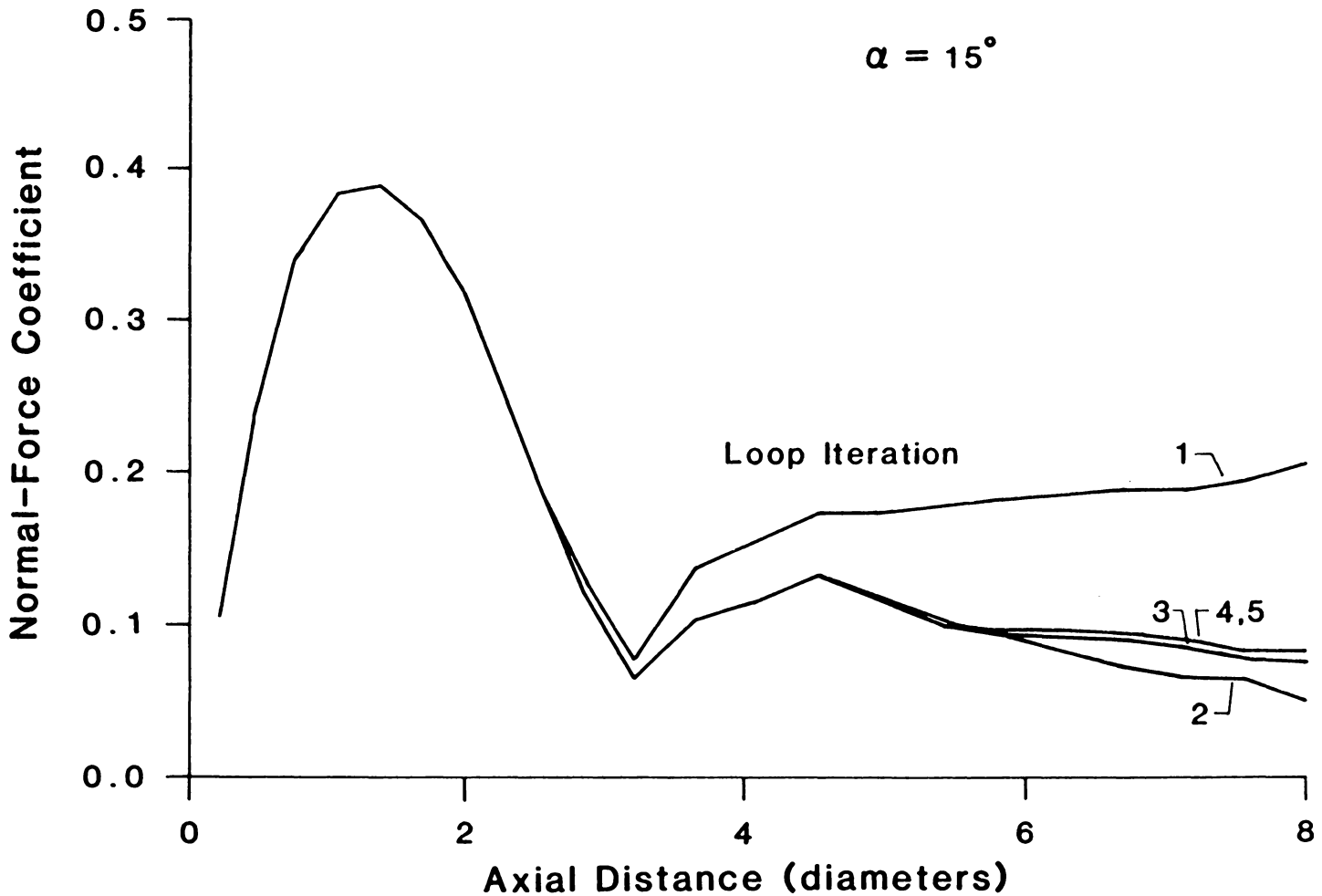

Figure 4-26 Convergence of normal-force coefficient with wake iteration

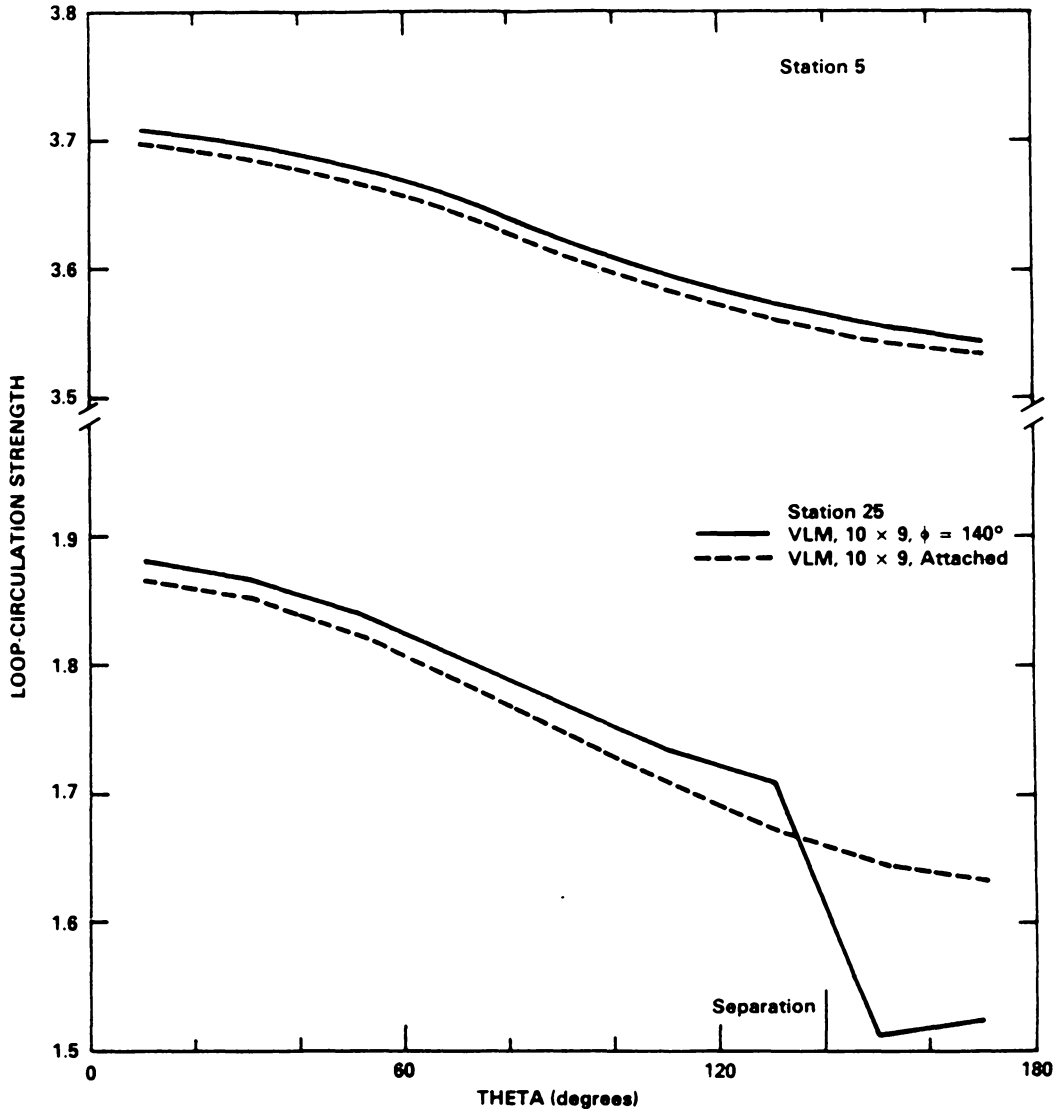

Figure 4-27 Circumferential variation of loop circulation strength for attached and separated flow at calculation stations 5 and 25.

The vita has been removed from the scanned document